AD-A099 440 CONSTRUCTION ENGINEERING RESEARCH LAB (ARMY) CHAMPAIGN IL F/6 20/1
BLAST NOISE PREDICTION, VOLUME I. DATA BASES AND COMPUTATIONAL --ETC(U
MAR 81 P D SCHOMER, L L LITTLE, D L EFFLAND

UNCLASSIFIED CERL-TR-N-98 NL

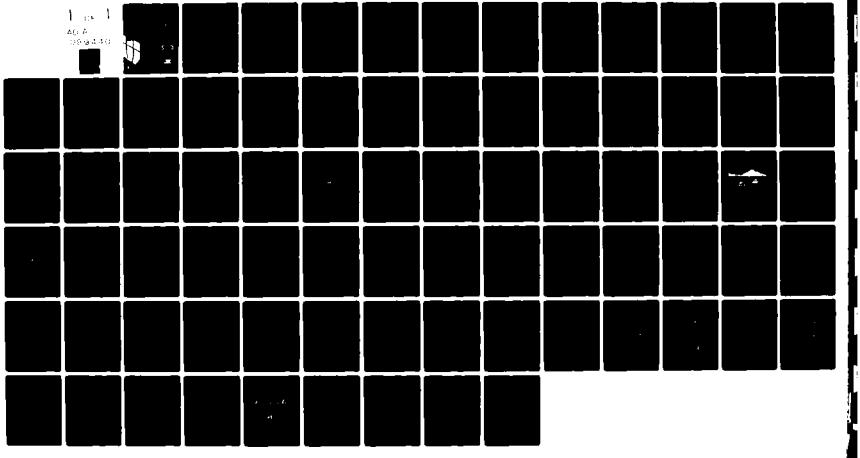

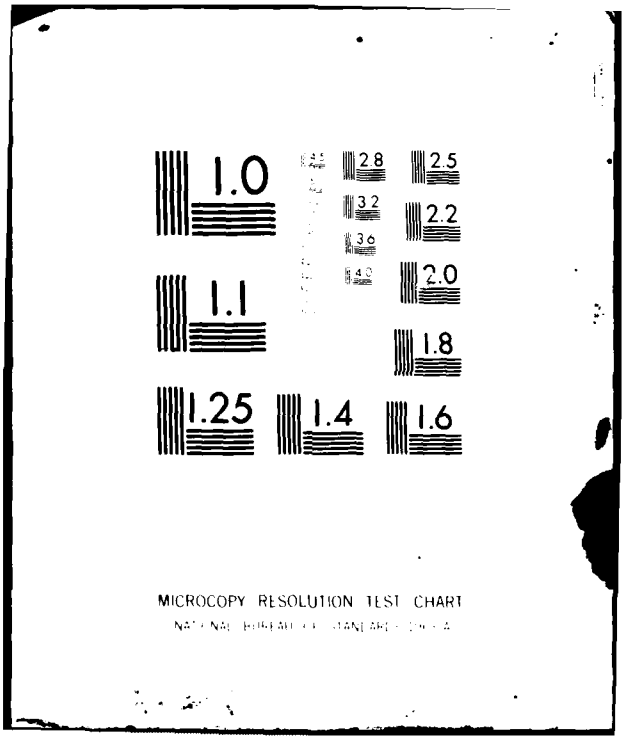
1.0
2.8
2.5
3.2
2.2
3.6
4.0
2.0
1.1
1.8
1.25
1.4
1.6
MICROCOPY RESOLUTION TEST CHART

construction engineering research laboratory

United States Army
Corps of Engineers
...Serving the Army
...Serving the Nation

TECHNICAL REPORT N-98
March 1981
Refined and Validated Noise Contour System

BLAST NOISE PREDICTION VOLUME I: DATA BASES AND COMPUTATIONAL PROCEDURES

(12) LEVEL III

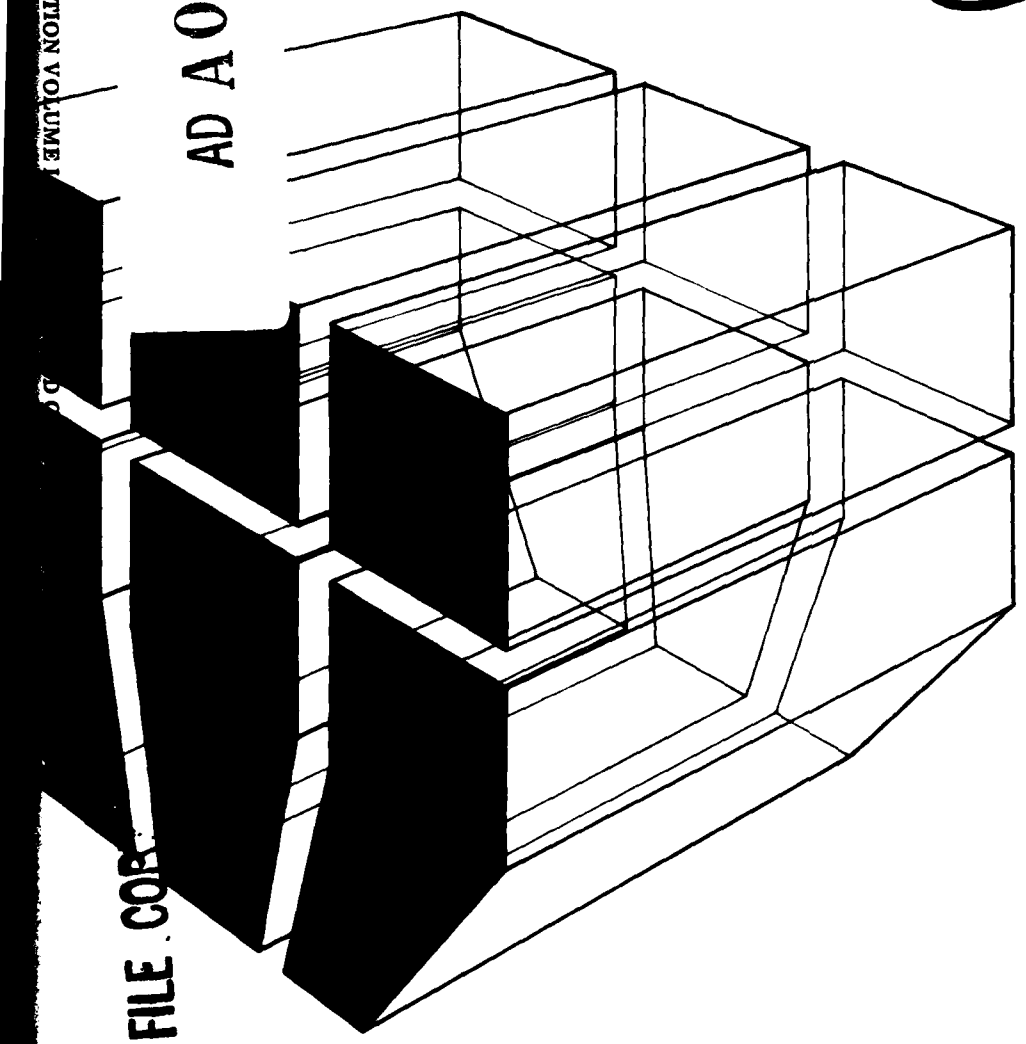

by
Paul D. Schomer
Lincoln L. Little
David L. Effland
Violet I. Pawlowska
Steven G. Roubik

CERL

BLAST NOISE PREDICTION VOLUME I

March 1981

UNCLASSIFIED

SECURITY CLASSIFICATION OF THIS PAGE (When Data Entered)

REPORT DOCUMENTATION PAGE

READ INSTRUCTIONS BEFORE COMPLETING FORM

1. REPORT NUMBER: CERL-TR-N-98	2. GOVT ACCESSION NO.: AD-A099440
3. RECIPIENT'S CATALOG NUMBER	
4. TITLE (and Subtitle): BLAST NOISE PREDICTION. VOLUME I. DATA BASES AND COMPUTATIONAL PROCEDURES. AD-A099335	5. TYPE OF REPORT & PERIOD COVERED: FINAL rept.
	6. PERFORMING ORG. REPORT NUMBER
7. AUTHOR(s): Paul D. Schomer, Violet I. Pawlowska, Lincoln L. Little, Steven G. Roubik, David L. Effland	8. CONTRACT OR GRANT NUMBER(s): 12 76
9. PERFORMING ORGANIZATION NAME AND ADDRESS: U.S. ARMY CONSTRUCTION ENGINEERING RESEARCH LAB, P.O. Box 4005, Champaign, IL 61820	10. PROGRAM ELEMENT, PROJECT, TASK AREA & WORK UNIT NUMBERS: 4A762720A896-A-012
11. CONTROLLING OFFICE NAME AND ADDRESS: 16 4A762720A896 17 A	12. REPORT DATE: 11 March 1981
	13. NUMBER OF PAGES: 72
14. MONITORING AGENCY NAME & ADDRESS (if different from Controlling Office)	15. SECURITY CLASS. (of this report): Unclassified
	15a. DECLASSIFICATION/DOWNGRADING SCHEDULE

16. DISTRIBUTION STATEMENT (of this Report)

Approved for public release; distribution unlimited

17. DISTRIBUTION STATEMENT (of the abstract entered in Block 20, if different from Report)

18. SUPPLEMENTARY NOTES

Copies are obtainable from the National Technical Information Service
Springfield, VA 22151

19. KEY WORDS (Continue on reverse side if necessary and identify by block number)

20. ABSTRACT (Continue on reverse side if necessary and identify by block number)

Over the past several years, the Construction Engineering Research Laboratory has gathered data from various sources dealing with blast noise generation and propagation and has performed several sets of field measurements designed to enhance this data base. These studies have been performed as a part of efforts aimed at improving methods of predicting the noise impact of military installations. Specifically included are measurements of the directivity pattern of major Army weapons and the statistical propagation of blast noise in the atmosphere. Volume I of this report develops and explains the relations

DD FORM 1 JAN 73 1473 EDITION OF 1 NOV 65 IS OBSOLETE

UNCLASSIFIED

405279 A

SECURITY CLASSIFICATION OF THIS PAGE (When Data Entered)

Item 20 continued.

among the various data bases which have been developed to predict blast noise impact of Army facilities. From these studies, data bases and computational procedures which are used within the Blast Noise Prediction computer program (BNOISE 3.2) are developed.

User instructions and a system description for the Blast Noise Prediction computer program, BNOISE 3.2, are given in Volume II. Also included is the procedure for using the program to obtain a noise contour for a specific set of data; how subroutines are invoked in a modular fashion; a description of module functions; module calling procedure; algorithms used by the program; and a summary of error messages.

FOREWORD

This research was conducted for the Directorate of Military Programs, Office of the Chief of Engineers (OCE), under Project 4A76270A896, "Environmental Quality for Construction and Operation of Military Facilities"; Task A, "Environmental Impact Monitoring Management Assessment and Planning"; Work Unit 012, "Refined and Validated Noise Contour System." The QCR number is 3.01.006. Mr. F. P. Beck, DAEN-MPE-I, is the OCE Technical Monitor.

The work was performed by the Environmental Division (EN), U.S. Army Construction Engineering Research Laboratory (CERL). Dr. R. K. Jain is Chief of EN.

COL Louis J. Circeo is Commander and Director of CERL, and Dr. L. R. Shaffer is Technical Director.

CONTENTS

TABLES

FIGURES

FIGURES (Cont'd)

FIGURES (Cont'd)

BLAST NOISE PREDICTION
VOLUME I: DATA BASES AND COMPUTATIONAL PROCEDURES

1 INTRODUCTION

Background

Over the past several years, the U.S. Army Construction Engineering Research Laboratory (CERL) has gathered data from various sources dealing with blast noise generation and propagation and has performed several sets of field exercises designed to further develop information regarding blast noise sources and the propagation of blast noise in the atmosphere. These CERL studies include measurements of the propagation of 735 five-pound charges set off at a central location at Fort Leonard Wood, MO,[1] measurements at Fort Sill on the directivity pattern of all of the Army's major weapons,[2] and small-scale studies at Fort Sill, OK and Fort Leonard Wood (Appendices A and B) designed to examine the weight relation between blast charge size and blast amplitude and duration. These studies were performed as a part of efforts aimed at developing approved methods of predicting the impact of blast noise at military installations. Data generated by these studies are used in the CERL-developed Blast Noise Prediction computer program (BNOISE 3.2), designed to predict the noise impact of military installations resulting from the blast-producing operations of armor, artillery, and demolition.

Purpose

The purpose of this report is to develop and explain the relations between and among various data developed to predict the blast noise impact of Army facilities, and from these data bases, to develop the computational procedures used within the Blast Noise Prediction computer program. This volume describes data bases and computational procedures.

Outline of Report

The present Blast Noise Prediction computer program implements several technical procedures and uses several data bases, e.g., tables containing the expected magnitude distribution of blasts propagated in the atmosphere. This report devotes separate chapters to each of the separate data bases or procedures, arranged so that later chapters build on data developed in earlier chapters.

Chapter 2 describes and explains the blast amplitude statistics derived from the first Fort Leonard Wood measurements; Appendix A describes the test itself and Appendix B contains intermediate results. Chapter 3 explains the procedures by which the present Department of Defense (DOD) cut-off (85 decibels [dB] C-weighted sound-exposure level [CSEL]) is implemented. Chapter 4 explains the method developed to translate the data base developed in Chapter 2 from one geographic location to another.

Appendix C contains an analysis of the effects of wind on blast propagation, and Appendix D contains a further analysis of meteorological effects and suggests possible improvements to the prediction method.

At Fort Leonard Wood, the standard signal source was a 5-lb charge of C-4 plastic explosive set off at ground level; at Fort Sill, the standard source was a 5-lb charge of C-4 set off 3 ft (0.9 m) above ground level. Chapter 5 develops the means to relate these data to one another. The weapon contours developed at Fort Sill are adapted for use by the computer program described in Chapter 6. Chapter 7

[1] P. D. Schomer, R. J. Goff, and L. M. Little, *The Statistics of Amplitude and Spectrum of Blasts Propagated in the Atmosphere*, Volumes I and II, Technical Report (TR) N-13/ADA033361 and ADA033646 (U.S. Army Construction Engineering Research Laboratory [CERL], November 1976).

[2] P. D. Schomer, L. M. Little, and A. B. Hunt, *Acoustic Directivity Patterns for Army Weapons*, Interim Report (IR) N-60/ADA066223 (CERL, October 1978).

examines the growth function of various blast parameters as a function of the weight of charge. Volume II of this report describes the Blast Noise Prediction computer program.

Mode of Technology Transfer

The program and documentation for the Blast Noise Prediction computer system will be available from the Department of the Army Assigned Responsible Agency (1981).

2 BLAST PROPAGATION STATISTICS

General

This chapter summarizes the results of measurements performed at Fort Leonard Wood. Basically, during these measurements, 735 five-pound charges of C-4 plastic explosive were set off at ground level at a central location. Simultaneous recordings were made at 1000 and 2000 ft (305 and 610 m) and at 1, 2, 5, 10, and 15 miles (2, 3, 8, 16, and 24 km). Concurrent with the acoustical tests and measurements, a special Federal Aviation Administration (FAA) airplane monitored and recorded pertinent meteorological data including wind speed and direction, temperature, and humidity. Figure 1 illustrates the test setup.

There were two acoustical data collection systems:

1. At 1000 and 2000 ft and 1 mile (305 and 610 m and 2 km), unmanned transducer stations were used. These devices all sent their data back to a central control van via land cables.

2. At 2, 5, 10, and 15 miles (3, 8, 16, and 24 km), manned measurement stations were used. Each of these stations contained its own special low-frequency recorder.

Equipment at the manned stations included a 1-in. microphone and wind screen, and a sound-level meter used to measure peak amplitudes and to act as a pre-amplifier for the low-frequency tape recorder. Equipment at the unmanned stations included a remotely adjustable pre-amplifier which powered its own 1/2-in. microphone. An FM-type tape recorder was used at the control van.

CERL Technical Report (TR) N-13, *Statistics of Amplitude and Spectrum of Blasts Propagated in the Atmosphere*, details the analysis and reduction of data from the manned stations and the analysis and reduction of meteorological data. Peak values were determined for these acoustical data and one-third-octave spectra were obtained using special laboratory instrumentation. Energy-weighted measures were then developed from the one-third-octave data. Appendix A describes the recording and analysis of the close-in, Fort Leonard Wood data, i.e., data from 1000 and 2000 ft and 1 mile (305 and 610 m and 2 km). These data were reduced to peak levels and various frequency-weighted energy levels without the intermediate step of developing the one-third-octave bands. This direct analysis was made possible by means of the CERL-developed environmental noise monitor, described in CERL TR N-41, *True-Integrating Environmental Noise Monitor and Sound-Exposure Level Meter*, Volumes I through IV.[3]

Amplitude Statistics

In CERL TR N-13, data were divided at each distance into different amplitude ranges. This distribution was done on the basis of the peak sound level; the data from TR N-13 is listed in Table 1. The initial data (by distance) were presented in the form of a distribution; natural breakpoints were then chosen. To develop smooth distribution functions, minor perturbations to these breakpoints were selected. (This process is more fully described in Chapter 4 of TR N-13).

Virtually the same process has been used in this chapter to divide close-in data into amplitude ranges and frequencies of occurrence. However, because the CSEL is currently the required measure for environmental assessments,[4] the TR N-13 data have been divided and analyzed in this chapter on the basis of the CSEL rather than peak level. Appendix B contains these new amplitude distributions along with an indication of the initial and final breakpoints. Figure 2 illustrates a typical C-weighted amplitude distribution. Table 2 contains CSEL statistics for the close-in data; in order to couple the

---

[3] A. Averbuch, et al., *True-Integrating Environmental Noise Monitor and Sound Exposure Level Meter*, Volume I, TR N-41/ADA060958 (CERL, May 1978); *Volume II: Wiring and Parts Lists, Parts Layouts, and Schematics*, ADA072002 (CERL, 1979); *Volume III: Microprocessor Program and Data Interface Description*, and *Volume IV: Mechanical Construction and Electrical Check-Out*, ADA083320 and ADA083321 (CERL, March 1980).

[4] *Environmental Protection, Planning in the Noise Environment*, Army Technical Manual (TM) 5-803-2, Air Force Manual (AFM) 19-10, and Navy Publication (NAVFAC) P-970 (Departments of the Air Force, Army, and the Navy, 15 June 1978); *An Installation Compatible Use Zones*, 32 CFR 256 (4 January 1977), and *Guidelines for Preparing Environmental Impact Statements*, Report of Working Group 69 (The National Research Council, Committee on Hearing, Bioacoustics, and Biomechanics Assembly of Behavioral and Social Sciences, 1977).

close-in and the far-out data* from the Fort Leonard Wood tests, peak data from the far-out stations have been converted to CSELs (Table 3).

For completeness, peak level data are presented for the same groupings as chosen for C-weighted, close-in data. Table 4 contains peak level (energy) averages which have been computed for data grouped as per Table 2. Figures 3 and 4 contain C-weighted amplitude information from Tables 2 and 3, by day and by night. Figures 5 and 6 contain the peak level amplitude distributions from the data contained in Tables 1 and 4, by day and by night. Several facts are notable about the curves in Figures 3 through 6:

1. For the lowest level range at far distances, the curves tend to flatten out; a dashed line shows the true direction of these data. The flattening occurs when levels are low enough to be in the noise floor of the instrumentation and/or ambient.

2. The lowest and highest amplitude range data tend to disappear at short distances. This is as expected. As the muzzle of the gun or the source of an explosion is approached, the amplitude level becomes more constant and independent of terrain or weather conditions. Beyond the point where measured data exist, these curves have been extended and shown as dashed lines converging at or near the source. They are shown as dashed lines because, although they may indeed exist, their likelihood of occurrence is so low that they were not measured during the Fort Leonard Wood tests. Thus, Table 2 lists these values with a percentage of 0. The point of convergence is chosen from the solid line on the figures. These solid lines are developed and shown in Figures 7 and 8 for peak and C-weighting, respectively. They represent a straight line fit (least squares) to the total (energy averaged) day and night data.

3. TR N-13 established that the "base" zone curve corresponds most nearly to sound propagated under a standard type of atmosphere. It is interesting to note that a best-fit straight line to these curves approaches the same value for the data by day and by night, further supporting the concept that, at the muzzle of a gun or at the source of a blast, the amplitudes are independent of weather or terrain.

4. The fact that the curves in Figures 3, 4, 5, and 6 show no great discontinuities indicates that there are no systematic differences either between the data gathered at the unmanned or manned stations or between any of the individual unmanned or manned distances. They thus serve as a good check on the overall validity of the data.

5. When the differences between peak levels averaged on an energy basis were compared to CSEL levels averaged on an energy basis, it was found that the differences (by day and by night) for the four amplitude groupings grow toward a 25-dB limit as distance decreases, i.e., multipaths cease to exist but shock wave remains, indicating a generally higher frequency content (Table 5).

* 2, 5, 10 and 15 miles (3, 8, 16, and 24 km).

Table 1
Statistics of Blast Propagation–Peak Sound-Pressure Level (Zone Averages) and Frequency of Occurrence (5 lb on Ground)

Time	Distance miles (km)	Zone 1* ExN	Zone 2* N	Zone 3* B	Zone 4* F
0500 to 0700 hours	2 (3.2)	93.0 dB 25.4%	105.1 dB 29.5%	114.6 dB 39.0%	121.9 dB 6.1%
	5 (8.0)	74.8 dB 33.8%	89.3 dB 31.3%	101.0 dB 27.3%	110.0 dB 7.6%
	10 (16.1)	72.8 dB 47.9%	83.8 dB 25.0%	95.1 dB 20.0%	105.8 dB 7.1%
	15 (24.1)	71.6 dB 45.2%	80.5 dB 33.7%	92.7 dB 16.7%	105.3 dB 4.4%
0700 to	2 (3.2)	95.7 dB 37.5%	105.9 dB 39.6%	114.3 dB 20.6%	123.0 dB 2.3%
	5 (8.0)	75.9 dB 29.5%	90.0 dB 35.0%	102.0 dB 25.9%	112.2 dB 9.6%
	10 (16.1)	71.1 dB 25.9%	83.1 dB 32.6%	95.0 dB 31.8%	105.3 dB 9.7%
	15 (24.1)	69.1 dB 34.8%	79.9 dB 32.1%	91.6 dB 30.0%	102.3 dB 3.1%

*Zone headings refer to the sound velocity profile:
ExN = Excess Negative
N = Negative
B = Base
F = Focus

Table 2
CSEL Zone Averages and Frequency of Occurrence (5 lb on Ground)

Time	Distance ft (m)	Zone 1* ExN	Zone 2* N	Zone 3* B	Zone 4* F
0500 to 0700 hours	1000 (304)	103.4 0.0%	115.3 72.66%	121.2 27.34%	127.3 0.0%
	2000 (610)	94.5 8.12%	104.2 44.21%	114.1 47.67%	121.2 0.0%
	5280 (1610)	79.5 7.15%	90.8 24.35%	101.5 65.86%	107.8 2.64%
0700 to 1100 hours	1000 (304)	103.0 2.24%	114.1 72.69%	121.9 25.07%	129.0 0.0%
	2000 (610)	93.9 8.34%	103.3 59.22%	113.6 32.44%	120.9 0.0%
	5280 (1610)	83.8 16.13%	94.2 64.88%	102.7 18.53%	110.2 0.46%

*Zone headings refer to the sound velocity profile:
ExN = Excess negative
N = Negative
B = Base
F = Focus

Table 3
CSEL Zone Averages Converted from Peak Data Zones in Table 1 (5 lb on Ground)

Night**	Distance miles (km)	Zone 1* ExN	Zone 2* N	Zone 3* B	Zone 4* F
(0500 to 0700 hours)	2 (3.2)	70.1	83.8	92.2	98.3
	5 (8.0)	57.4	70.3	81.6	88.6
	10 (16.1)	56.1**	65.3	75.7	84.9
	15 (24.1)	54.9**	61.8	73.0	83.5
Day**					
(0700 to 1100 hours)	2 (3.2)	74.0	82.8	91.3	99.4
	5 (8.0)	57.4	70.7	82.0	91.0
	10 (16.1)	53.9**	66.3	76.6	84.4
	15 (24.1)	53.1**	62.7	72.7	81.6

*Zone headings refer to the sound velocity profile:
ExN = Excess negative
N = Negative
B = Base
F = Focus

**The values used by the computer are:
Night: 10 miles (16.1 km) = 52.0; 15 miles (24.1 km) = 48.5
Day: 10 miles (16.1 km) = 51.5; 15 miles (24.1 km) = 46.0

Table 4
Peak Level Zone Averages for Zones in Table 2 (5 lb on Ground)

Time	Distance ft (m)	Zone 1* ExN	Zone 2* N	Zone 3* B	Zone 4* F
0500 to 0700 hours	1000 (305)	131.5	139.7	144.5	148.0
	2000 (610)	119.3	128.6	137.3	143.0
	5280 (1610)	104.7	115.4	125.0	132.9
0700 to 1100 hours	1000 (305)	127.9	137.9	145.6	149.0
	2000 (610)	118.3	127.0	136.5	144.0
	5280 (1610)	109.5	118.1	126.0	134.4

*Zone headings refer to the sound velocity profile:

ExN = Excess negative
N = Negative
B = Base
F = Focus

Table 5
Peak Level Minus CSEL by Distance and Propagation Group

Time	Distance	Zone 1* ExN	Zone 2* N	Zone 3* B	Zone 4* F
0500 to 0700 hours	1000 ft (305 m)	25.5**	24.4	23.30	23.5**
	2000 ft (610 m)	24.8	24.4	23.20	24.5**
	1 mile (1.6 km)	25.2	24.6	23.10	22.1
	2 miles (3.2 km)	22.9	21.3	22.4	23.6
	5 miles (8.0 km)	17.4	19.0	19.4	21.4
	10 miles (16.1 km)	16.7	18.5	19.4	20.9
	15 miles (24.1 km)	16.7	18.7	19.7	21.8
0700 to 1100 hours	1000 ft (305 m)	24.9	23.7	23.7	24.0**
	2000 ft (610 m)	24.4	23.7	22.9	25.5**
	1 mile (1.6 km)	25.7	23.9	23.3	24.2
	2 miles (3.2 km)	21.7	23.1	23.0	23.6
	5 miles (8.0 km)	18.5	19.3	20.0	21.2
	10 miles (16.1 km)	17.20	16.8	18.4	20.9
	15 miles (24.1 km)	16.0	17.2	18.9	20.7

* Zone headings refer to the sound velocity profile:
ExN = Excess Negative
N = Negative
B = Base
F = Focus

**Extrapolated from the extended curves.

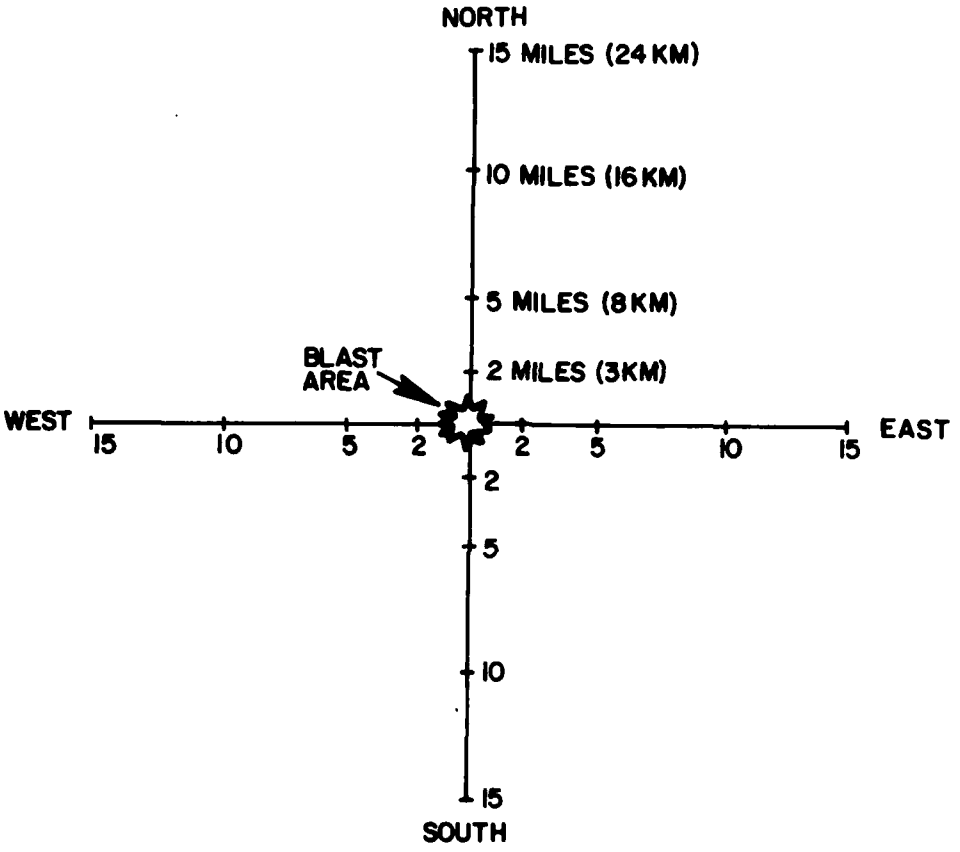

Figure 1. Array of measurement stations.

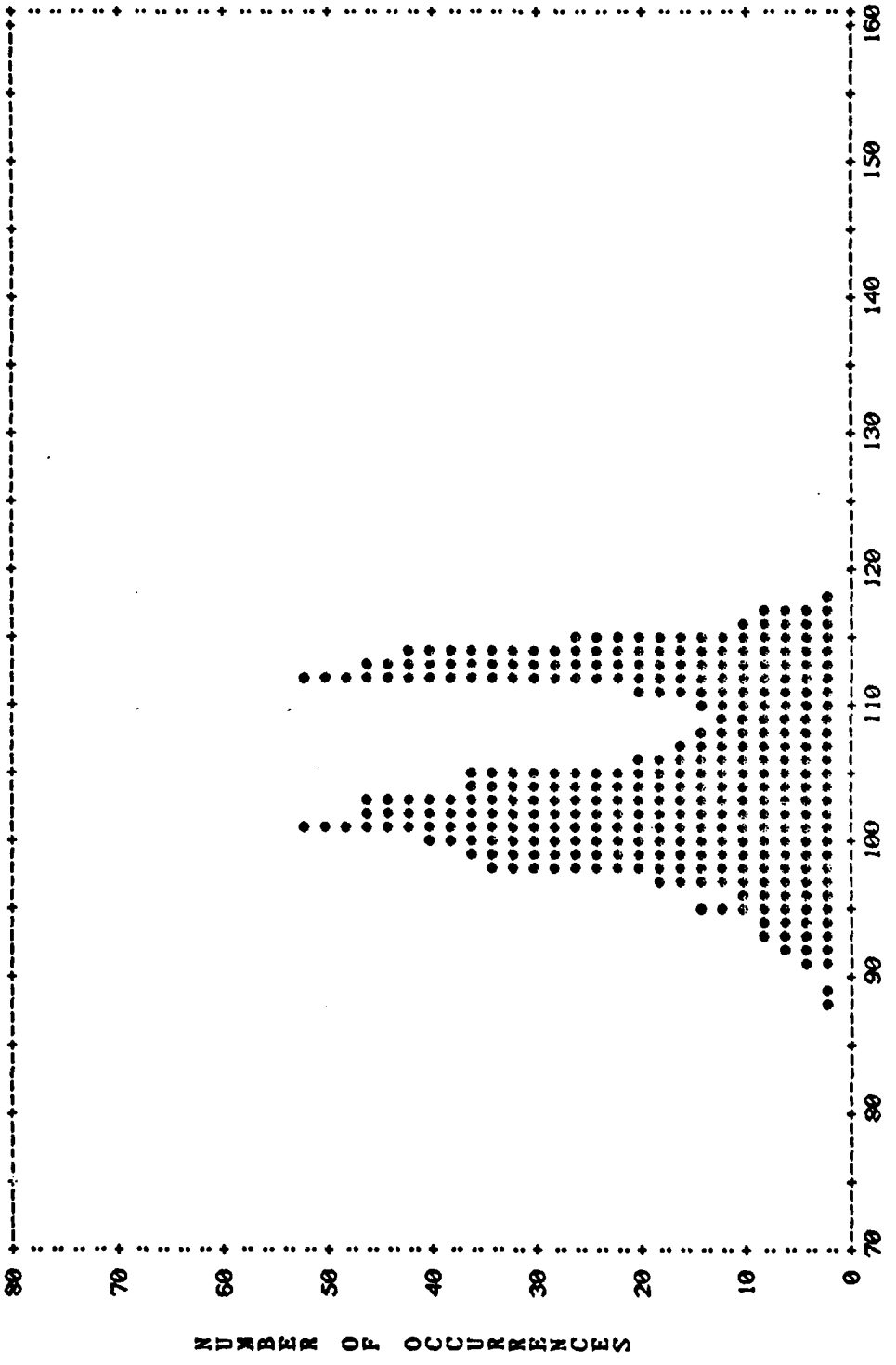

Figure 2. CSEL (dB) distribution of received data at 2000 ft.

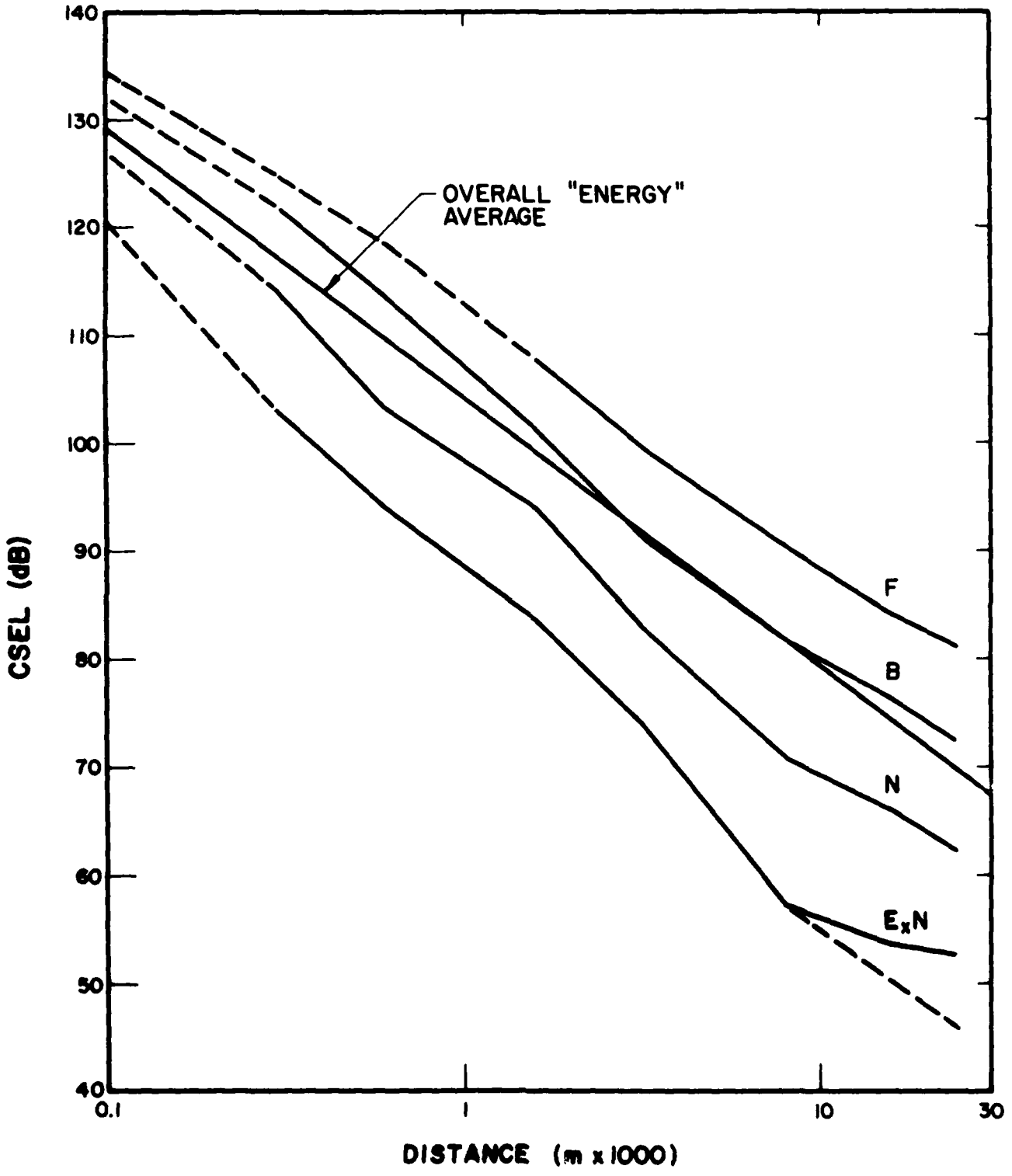

Figure 3. CSEL vs distance (day).

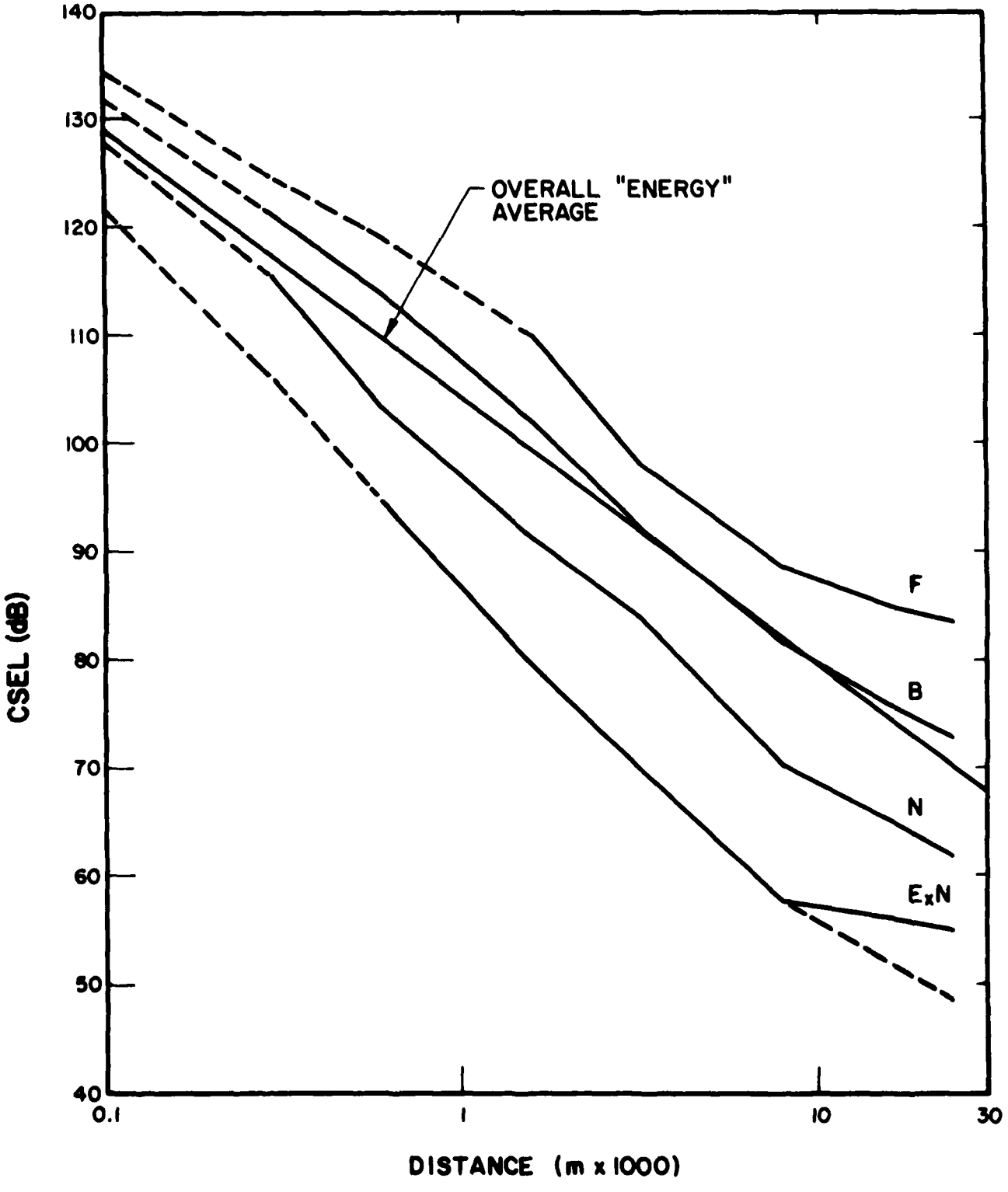

Figure 4. CSEL vs distance (night).

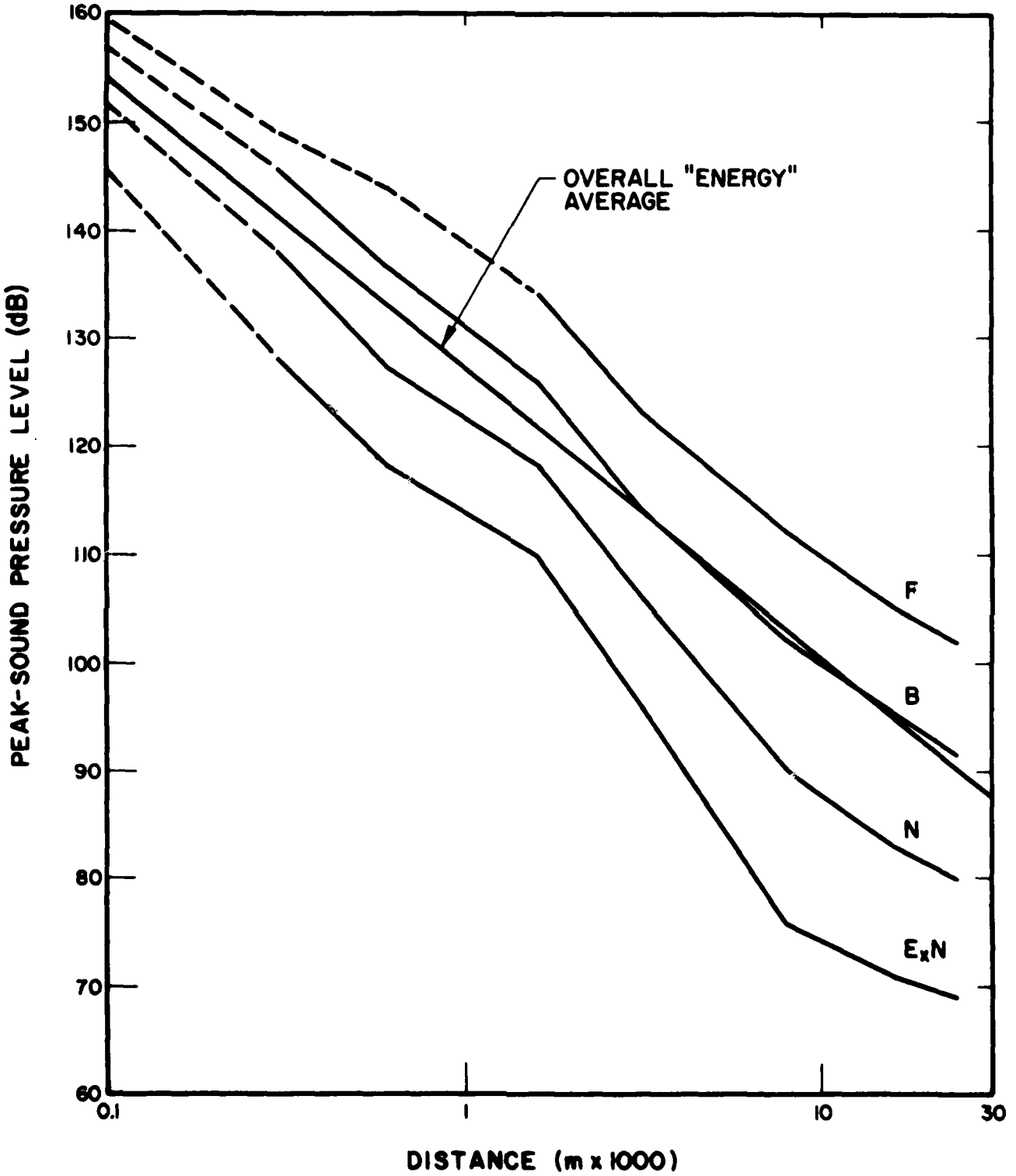

Figure 5. Peak sound-pressure level vs distance (day).

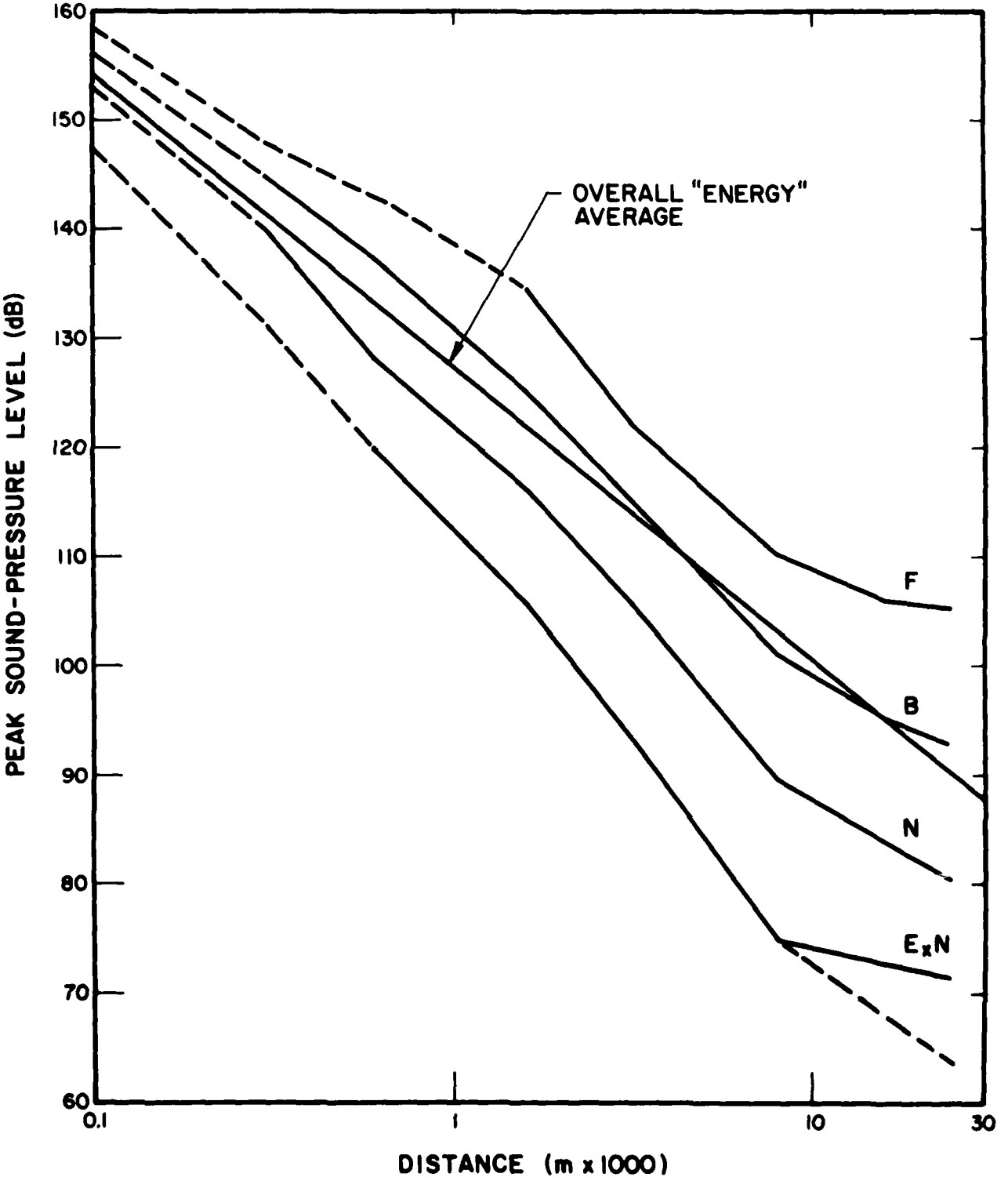

Figure 6. Peak sound-pressure level vs distance (night).

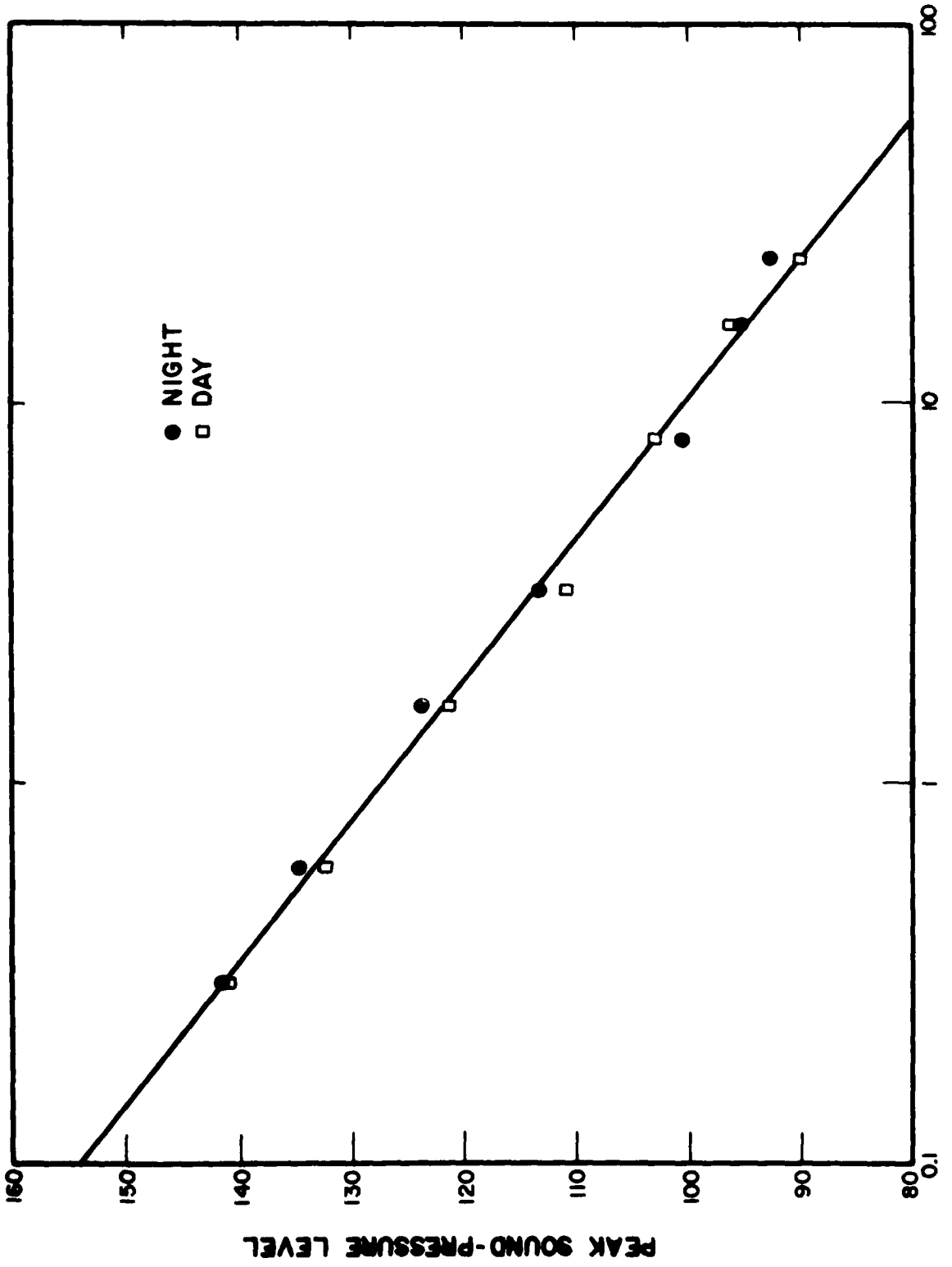

Figure 7. Peak sound-pressure level vs distance (all "energy" data averaged together).

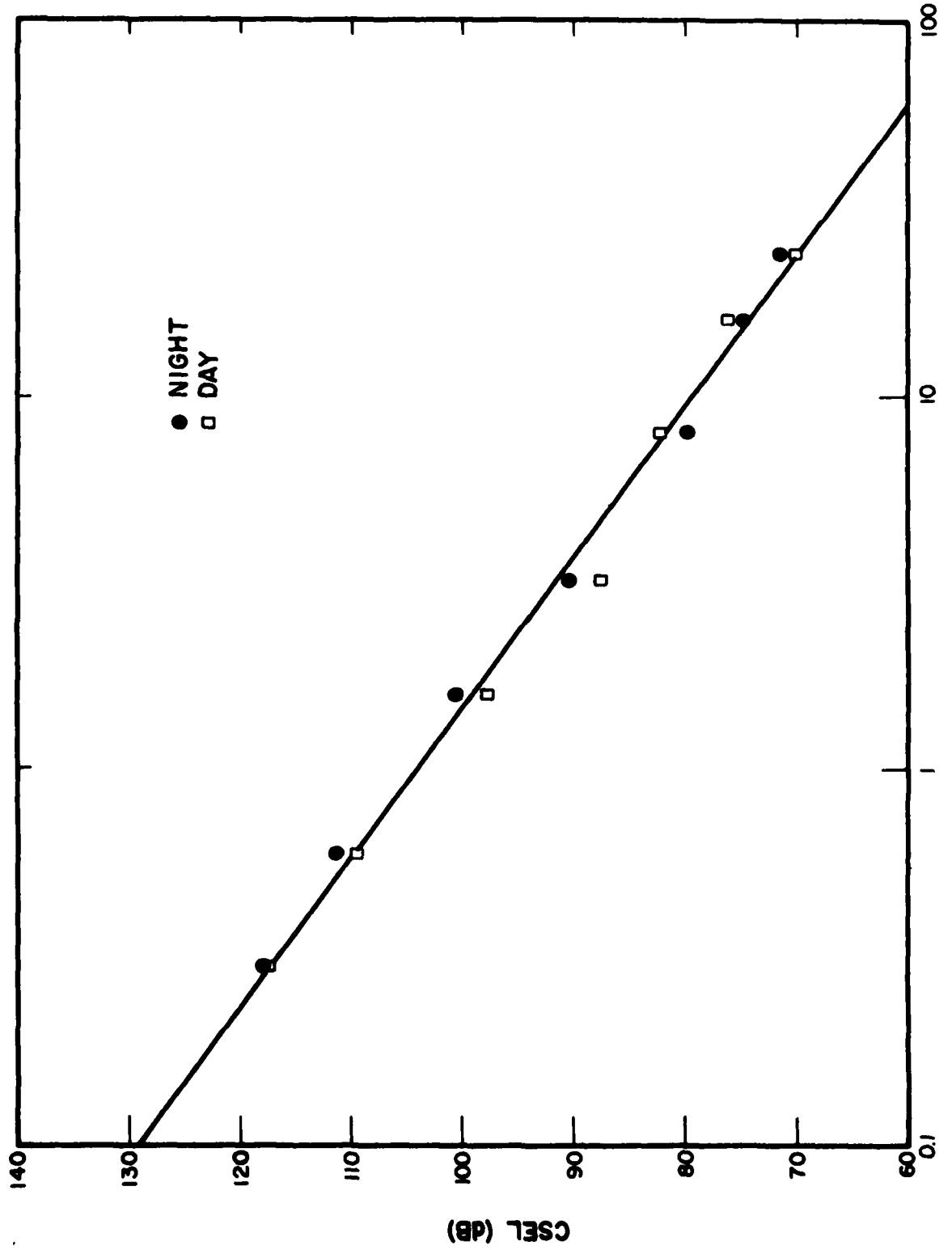

Figure 8. CSEL vs distance (all "energy" data averaged together).

3 IMPLEMENTATION OF A HIGH-AMPLITUDE REQUIREMENT

In Chapter 2, distribution data were developed (Tables 2 and 3) which provided amplitudes and frequencies of occurrence for CSELs in four blast magnitude ranges. These data alone are enough to predict the total CSEL impinging on any point in space; they are also flexible enough to indicate near maximum levels and to allow for the inclusion of some type of "impulse correction factor" should that be deemed desirable in the future. However, current procedures used by DOD and the National Academy of Science require the exclusion of all data having CSELs below a given threshold.[5] Currently, the threshold is 85 dB during the day and 75 dB at night. The purpose of this chapter is to consider and develop means to implement a threshold requirement given the data base developed in Chapter 2.

To implement a threshold requirement given the data developed in Chapter 2, it is necessary to not only specify the mean sound-exposure level (SEL) values for a given magnitude range (along with frequency of occurrence), but also to describe the extent or boundaries of these magnitude ranges. Table 6 lists the breakpoints or zone end points used to divide the C-weighted close-in data into its four zones. Table 6 includes breakpoints and endpoints for range 1 and 4 data for which the frequency of occurrence is 0. These extensions are provided only for completeness and convenience within the computer program within which they are ultimately used, since they occur (in Table 2) with a probability of 0.

As discussed in Chapter 2, TR N-13 far-out data (i.e., data gathered at 2, 5, 10, and 15 miles [3, 8, 16, and 24 km]) were divided and portrayed on the basis of peak amplitudes rather than CSEL (Table 7). Given the peak amplitude and the CSEL differences for the various range amplitudes derived in Chapter 2, these breakpoints have been converted to CSEL on a proportional basis. For example, for 5 miles (8 km) daytime, the focus or range 4 peak amplitude (Table 1) is 112.2 dB and the base or range 3 amplitude is 102.0 dB. The corresponding mean CSELs are 91.0 and 82.0 (Table 3) for peak minus C-weighted differences of 21.2 and 20.0 (Table 5). The peak breakpoint between these two ranges given by Table 7 was 106.5 dB. This peak value is converted to a CSEL by the following formula:

$$CSEL\ BOUNDARY\ (i,i-1) = Peak\ Boundary\ (i,i-1) - (PC(i)+PC(i-1))/2 \qquad \text{[Eq 1]}$$

where PC(i) is the peak level minus the CSEL for the ith range.

Using this formula, the data from Table 7 have been converted to CSELs and presented in Table 8. As with Table 6, Table 8 includes endpoints for range 1 and 4 data. Figures 9 and 10 combine data from Tables 6 and 8, plotted as a function of distance. These figures also indicate the mean SEL within the described ranges.

To implement a threshold cutoff requirement, the data in any range must be analytically modeled; i.e., the frequency distributions represented by histograms such as Figure 2 must be analytically approximated. Within any of the four magnitude ranges, the simplest amplitude distribution function that can be considered is a constant. Figure 11 illustrates the data taken from the base day amplitude magnitude range of Figure 2, plus a constant amplitude distribution used to approximate these data. This constant is selected such that the total number of events represented by the range remains invariant. The total sound exposure, E, is given by

$$E = \int_a^c \eta(L_E) 10^{L_E/10} dL_E \qquad \text{[Eq 2]}$$

where $\eta(L_E)$ is the density of events as a function of SEL L_E.

[5] *Environmental Protection, Planning in the Noise Environment*, TM 5-803-2, AFM 19-10, and NAVFAC P-970 (Departments of the Air Force, Army, and the Navy, 15 June 1978); *Air Installation Compatible Use Zones*, 32 CFR 256 (4 January 1977), and *Guidelines for Preparing Environmental Impact Statements*, Report of Working Group 69 (The National Research Council, Committee on Hearing, Bioacoustics, and Biomechanics Assembly of Behavioral and Social Sciences, 1977).

Letting

$$\int_a^b 10^{L_I/10} dL_E = \bar{E}_A \qquad \text{[Eq 10]}$$

$$\int_b^c 10^{L_I/10} dL_E = \bar{E}_C \qquad \text{[Eq 11]}$$

and solving Eq 8 and 9 yields

$$\eta_1 = \frac{N(\bar{E}_C - C\bar{E})}{\bar{E}_C A - \bar{E}_A C} \qquad \text{[Eq 12]}$$

and

$$\eta_2 = \frac{N(\bar{E}_A - A\bar{E})}{\bar{E}_C A - \bar{E}_A C} \qquad \text{[Eq 13]}$$

Now, using η_1 and η_2, the total sound exposure E_N, above any arbitrary value L_o, can be calculated approximately for the following cases:

1. $L_o < a$
2. $a < L_o < b$
3. $b < L_o < c$
4. $L_o > c$

In Case 1, if $L_o < a$, then $E_N = E$.

In Case 2, if $a < L_o < b$, then

$$EN = E - \eta_1 \int_a^{L_o} 10^{L_I/10} dL_E. \qquad \text{[Eq 14]}$$

In Case 3, $b < L_o < c$ then

$$E_N = \eta_2 \int_{L_o}^{c} 10^{L_I/10} dL_E \qquad \text{[Eq 15]}$$

In Case 4, $L_o > c$ then $E_N = 0$.

The total number of events N is given by

$$N = \int_a^c \eta(L_E)\, dL_E \qquad \text{[Eq 3]}$$

and the average sound exposure per event is

$$\bar{E} = E/N \qquad \text{[Eq 4]}$$

If η_o approximates $\eta(L_E)$ such that

$$N = \eta_o(b-a) \qquad \text{[Eq 5]}$$

then

$$E_o = \eta_o \int_a^c 10^{L_I/10}\, dL_E \qquad \text{[Eq 6]}$$

and

$$\bar{E}_o = E_o/N \qquad \text{[Eq 7]}$$

which is not necessarily or generally equal to $\bar{E}$.

Eqs 2 through 7 show that a single constant frequency distribution allows the number of events to remain invariant, but does not allow any means to simultaneously adjust both the total sound exposure and the number of events represented by the distribution. Thus, a somewhat more complex model is required -- a model which holds both the number of events invariant and keeps the total energy within a range invariant requires a distribution represented by two constants. One of these constants is for data lying below the (energy) mean SEL value, and the other is for data lying above the (energy) mean SEL value.

The two-constant approximate distribution is shown in Figure 12 for the same data as Figure 11. If two frequency distribution constants, η_1 and η_2, are provided, both the total sound exposure and total number of events can be kept invariant. The following equations solve for η_1 and η_2 in terms of (1) the magnitude range and levels, (2) the total sound exposure represented by the magnitude range, and (3) the number of events represented by the magnitude range. Once these values are obtained, it is a simple matter to determine the total sound exposure for events lying above any given threshold.

Eqs 2, 3, and 4 show how E, N, and $\bar{E}$ can be calculated. In this case, however, if one approximates $\eta(L_E)$ by η_1 and η_2, then one can require that both

$$N = \eta_1 A + \eta_2 C \qquad \text{[Eq 8]}$$

where A = b-a and C = c-b

and that

$$E = \eta_1 \int_a^b 10^{L_I/10}\, dL_E + \eta_2 \int_b^c 10^{L_I/10}\, dL_E \qquad \text{[Eq 9]}$$

Eqs 8 and 9 are two equations in two unknowns, η_1 and η_2.

Table 6
CSEL Range Boundaries at 1000 and 2000 ft and 1 mile (5 lb on Ground)

Time	Distance ft (m)	Range 1* ExN		Range 2* N		Range 3* B		Range 4* F
		MIN	MAX/MIN		MAX/MIN		MAX/MIN	MAX
0500 to 0700 hours	1000 (305)	97.7	105.5		118.5		125.5	129.0
	2000 (610)	86.0	96.5		108.5		119.5	124.0
	5280 (1610)	72.0	83.5		95.5		109.5	112.8
0700 to 1100 hours	1000 (305)	94.0	104.5		118.5		128.5	129.0
	2000 (610)	87.6	96.5		109.5		120.5	123.5
	5280 (1610)	75.5	87.5		98.5		108.5	114.2

*Range headings refer to the sound velocity profile:

ExN = Excess negative
N = Negative
B = Base
F = Focus

Table 7
Peak Level Range Boundaries at 2, 5, 10, and 15 miles (5 lb on Ground)

Time	Distances mile (km)	Extension of Values (dB) Range 1* (ExN)	Range 2* (N)	Range 3* (B)	Range 4* (F)
Night	2 (3.2)	50–97	98–109	110–119	120–135
	5 (8.0)	50–80	81–93	94–106	107–135
	10 (16.1)	50–76	77–88	89–100	101–135
	15 (24.1)	50–73	74–83	84–97	98–135
Day	2 (3.2)	50–100	101–109	110–119	120–135
	5 (8.0)	50–80	81–95	96–106	107–135
	10 (16.1)	50–73	74–87	99–100	101–135
	15 (24.1)	50–70	71–83	84–97	98–135

*Range headings refer to the sound velocity profile:

ExN = Excess negative
N = Negative
B = Base
F = Focus

Table 8
CSEL Range Boundaries at 2, 5, 10, and 15 miles (5 lb on Ground)

Time	Distance ft (m)	Range 1* ExN		Range 2* N		Range 3* B		Range 4* F
		MIN	MAX/MIN	MAX/MIN		MAX/MIN		MAX
0700 to 0500 hours	2 (3.2)	61.0	75.4	87.7		96.5		103.3
	5 (8.0)	47.5	62.3	74.3		86.1		93.6
	10 (16.1)	41.5	58.9	69.6		80.4		89.9
	15 (24.1)	37.5	55.3	64.3		76.8		88.5
0700 to 1100 hours	2 (3.2)	65.0	78.1	86.5		96.2		104.4
	5 (8.0)	47.5	61.6	75.9		85.9		96.0
	10 (16.1)	41.0	56.5	69.9		80.9		89.4
	15 (24.1)	35.0	53.9	65.5		77.7		86.6

*Range headings refer to the sound velocity profile:

Exn = Excess negative
N = Negative
B = Base
F = Focus

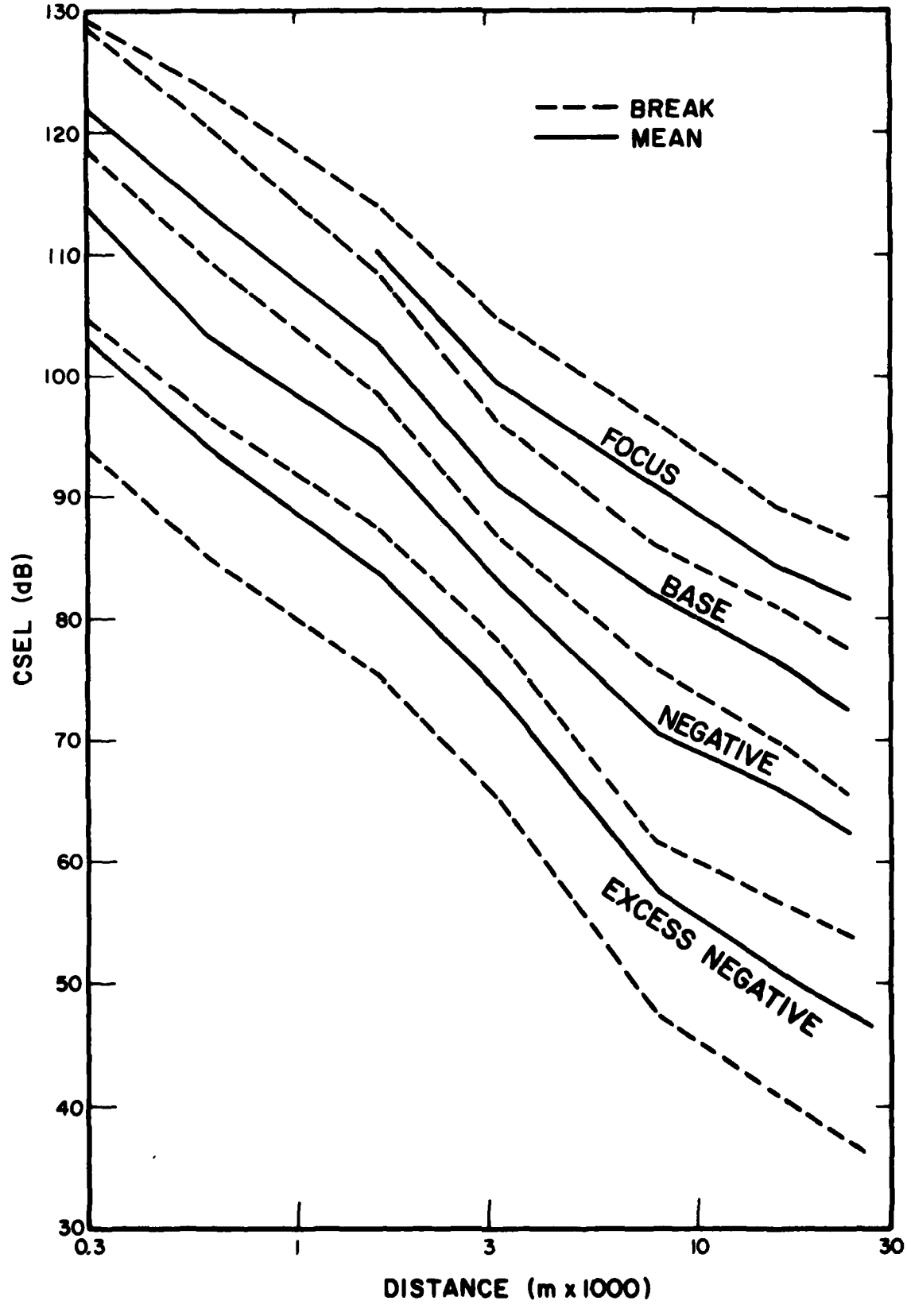

Figure 9. Means and break (day).

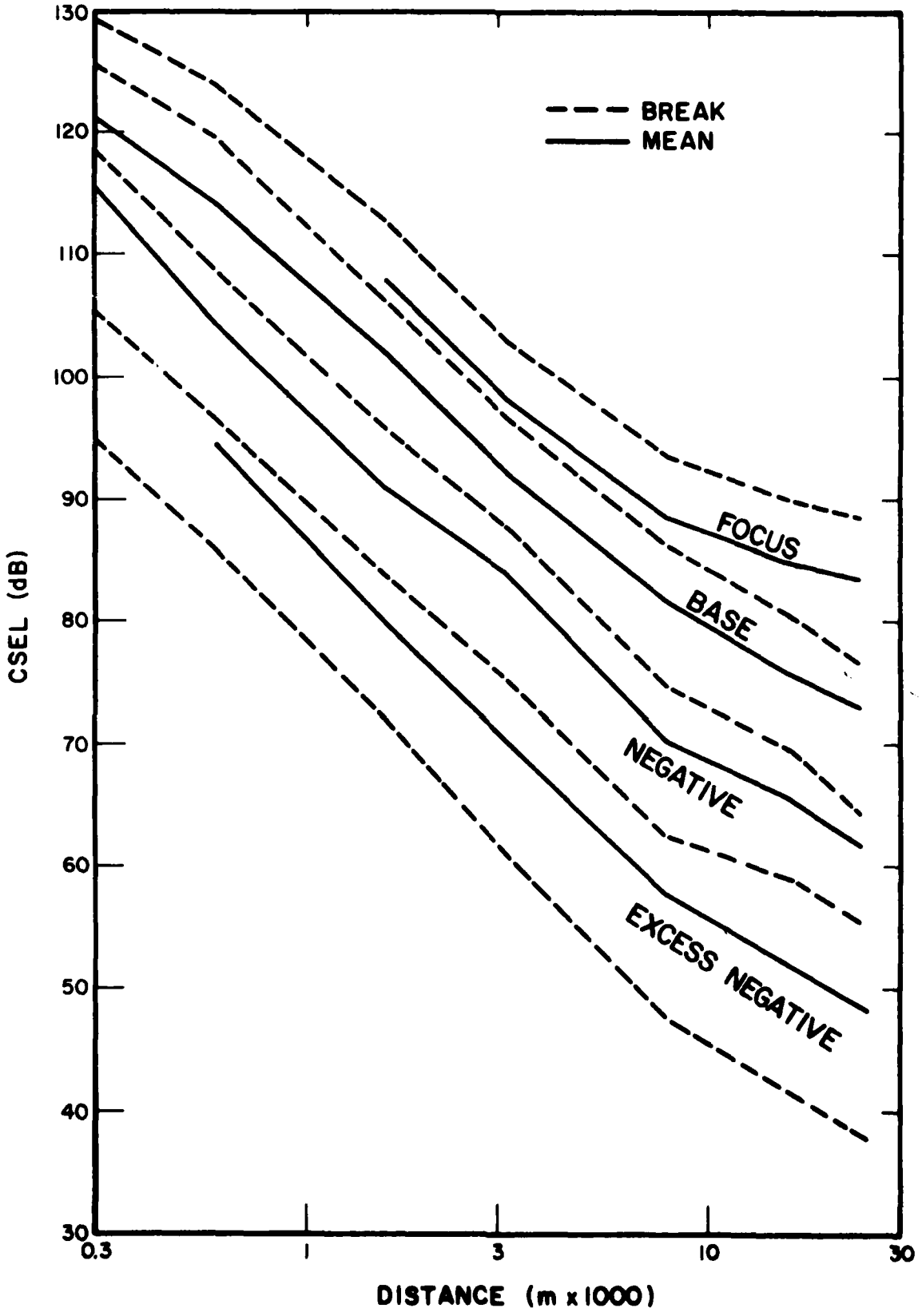

Figure 10. Means and break (night).

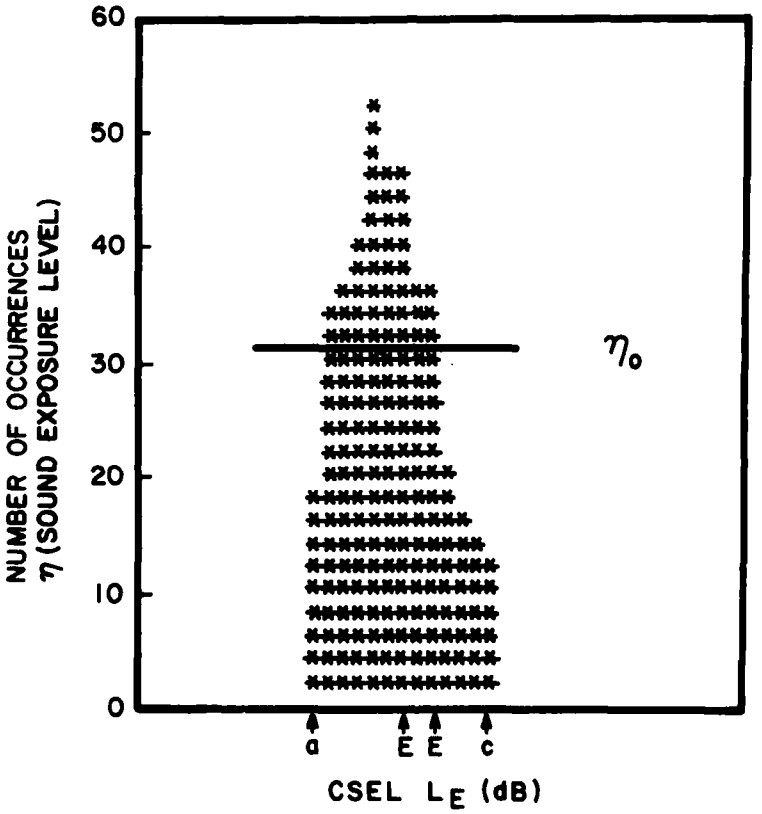

Figure 11. Approximation of a distribution range by a single constant.

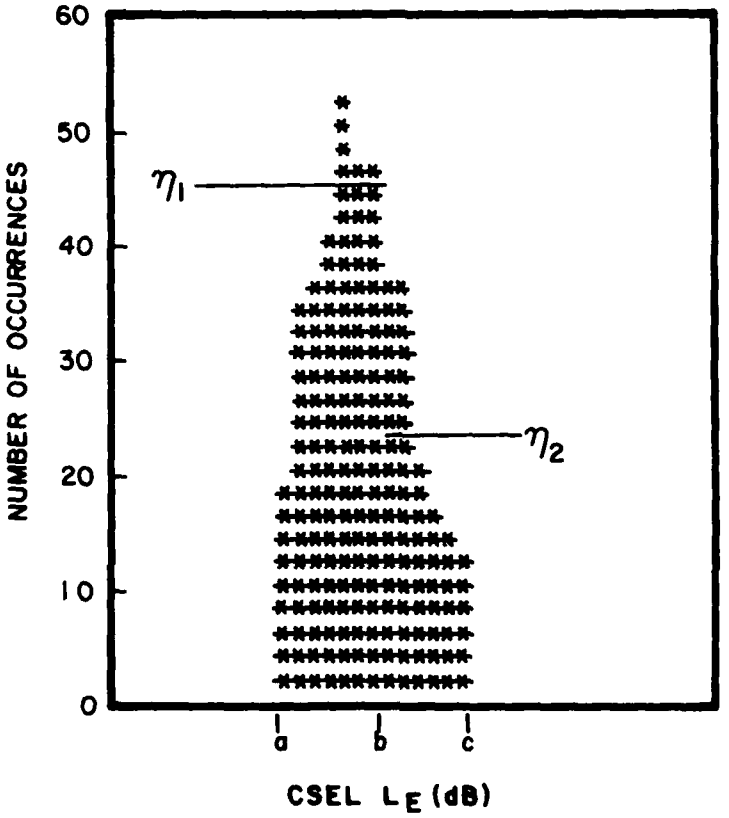

Figure 12. Approximation of a distribution range by two constants.

4 DEPENDENCE OF PROPAGATION STATISTICS ON LOCAL CLIMATE

In Chapter 2, magnitude range statistics were developed for data gathered at Fort Leonard Wood; in Chapter 3, means were developed for instituting a threshold or cutoff within computational procedures used to predict environmental noise impact. Since the data in Chapter 2 represent measurements made over approximately a 4-week period in the spring of 1973, it is necessary to develop procedures whereby these data can be generalized to other geographic regions and other times of the year.

CERL TR N-13 established the dependency of the four amplitude ranges on meteorological conditions. Specifically, the "focus" range occurred during conditions when the sound velocity underwent a double inversion; i.e., it first decreased with altitude, then increased with altitude, and then again decreased with altitude. "Base" or range 2 conditions occurred when there was a very weak focus or under conditions of a single inversion; i.e., when the sound velocity first increased with altitude and then began to decrease with altitude at some upper level. The lower level data (ranges 3 and 4) occurred when the sound velocity profile decreased with altitude or within the shadow region of a focus. Thus, one of the ingredients in translating the Fort Leonard Wood data to other locations and to other times of the year is knowledge of the long-term statistics relating to the sound velocity gradient.

The sound velocity gradient is approximately given as a linear function of temperature and wind. Unfortunately, since wind is a vector, it is different in different directions.

The weather bureau has gathered upper atmosphere statistics at approximately 50 sites spread more or less evenly throughout the continental United States. These statistics separately categorize temperature inversion frequencies of occurrence and gradients, and wind direction gradients and velocities.

There is no known, clearcut way of combining the weather bureau's temperature and wind data into sound velocity profiles which can be used to form data-translation equations. Appendix D contains a possible approach to this combinational problem, but requires a significantly larger data base gathered from several additional sites for validation and refinement. Additional measurements of the type carried out at Fort Leonard Wood will be performed at other locations which will provide different types of terrain and meteorological conditions. These data will lead to a more sophisticated model.

Results from CERL TR N-13 do make clear the fact that there is no simple relation between wind direction and received sound magnitude. Appendix C correlates CERL TR N-13 data with wind direction, and shows that early in the day at the more distant stations, the upwind direction is consistently the louder direction. Later in the day at shorter distances, the downwind directions exhibit the greater amplitudes.

Because of the ambiguity between upwind and downwind conditions, and because prevailing winds typically change with season (yearly contours are normally the type created), it has been decided at the present time to only use the temperature inversion statistics to develop data-translation equations. Clearly, when more is learned and the data base is enlarged, these temperature-based translations can possibly be modified to better reflect the contributions of the wind factor.

Current translation procedures have been developed based on temperature inversion statistics. Weather bureau data are gathered nationwide at 0000 and 1200 Greenwich Mean Time (which translates to 5 AM and 5 PM Central Daylight Time [CDT]). For the purposes of this report, only the 5 AM data are used, since these data correspond to the time period during which the Fort Leonard Wood measurements were performed, and since the analysis which follows indicates that this is the most reasonable data of the two available to use.

Examination of the far-out data (2, 5, 10, and 15 miles [3, 8, 16, and 24 km]) shows that the occurrence of focus situations typically sweeps out in distance as a function of time. This phenomenon occurs because as the normal nighttime inversion "burns off," it rises up from ground level and dissipates. Occasionally, low cloud layers (above which a sharp temperature inversion occurs) or strong wind shears constitute a reflecting layer. However, since the early morning inversions typically sweep out in space as a function of time and are related to the nighttime and early morning inversions, the early morning inversion frequency was chosen as the translation factor for daytime use. The assertion is made that the probability of a daytime focus is proportional to the probability of an early morning, nighttime inversion.

The early morning nighttime inversion frequency of occurrence (ground level to 500 ft [152 m]) was gathered from the weather bureau data for the season during which the Fort Leonard Wood measurements were made. The ratio at any location and for any season to these occurrence values for the Fort Leonard Wood area is used to translate the daytime statistics from one location and season to another. Specifically, the ratio R_D of early morning inversions at an altitude of 0 to 500 m at the location in question over the entire year or season in question as compared to these data at Fort Leonard Wood is used as a factor to multiply the frequency of range 3 or range 4 data and is given by

$$R_D = \frac{INV1 + INV2}{INV1_0 + INV2_0} \qquad \text{[Eq 16]}$$

where INV1 is the ground level and INV2 is the 1 to 500 m inversion frequencies at the site in question; $INV1_0$ and $INV2_0$ refer to these same quantities at Fort Leonard Wood for the period of the tests.

The amount by which range 3 or range 4 is increased (or decreased) is, on a proportional basis, subtracted from (or added to) the negative and excess negative data.

Nighttime conditions fall into two categories:

1. Simple, single, ground-level temperature inversions which are typical of clear nights. This type of condition will affect sound propagation at relatively short distances -- perhaps 5 miles (8 km) or less.

2. Higher level inversions and double inversions exist at some frequency of occurrence, and will cause large magnitudes to be received at greater distances -- typically greater than 5 miles (8 km). This last factor is probably the least well understood.

To accommodate these two conditions, two conversion factors were developed for nighttime -- one for distances of 2 miles (3 km) or less and the other for distances of 10 miles (16 km) or greater. A linear function was then fit between these two points.

For distances of 2 miles (3 km) or less, the frequency of ground-level inversion at the site and during the season in question, INV1, is compared as a ratio R_2 to the values during the test at Fort Leonard Wood. This ratio is used as a simple multiplier, as outlined for the daytime multiplier described above. Specifically:

$$R_2 = \frac{INV1}{INV1_0} \qquad \text{[Eq 17]}$$

The 10-mile (16-km) multiplication factor is given by the equation:

$$R_{10} = [(INV3 - INV3_0)/2 + INV3_0]/INV3_0 \qquad \text{[Eq 18]}$$

where INV3 is the new location inversion frequency from 1 to 3000 m and $INV3_0$ is this same frequency for the time period of the Fort Leonard Wood tests.

Eq 18 is based on an inversion frequency up to an altitude of 2000 ft (610 m); because of the uncertainty, it includes a factor of one-half in the multiplier to make the results less sensitive to large changes.

Typically, the variations in these inversion frequencies from one location to another and from one season to another are not very large. Thus, these translation factors do not play a great role in the overall noise predicted for a facility. Fort Leonard Wood is in the Missouri Ozarks, an area typical of the type of terrain over much of the continental United States. In mountainous areas or on seacoasts where special conditions exist, there is some reason to believe that other factors will increase the inversion frequency and increase the occurrence of large amplitude events over what is predicted by these translation factors. However, there are no data to substantiate that these other factors are present.

5 BLAST GENERATION -- GROUND EFFECTS

The measurements at Fort Leonard Wood indicated a small degree of data variability caused by unequal soil motions from one blast to another. To mitigate this variability, subsequent measurements were performed using 5-lb charges of C-4 plastic explosive placed on a post raised 3 ft (0.9 m) above ground level. Thus, to compare data developed from above-ground tests with the amplitude statistics developed from measurements made at ground level, it is necessary to develop an appropriate conversion factor.

The measurements at Fort Sill are described in CERL TR N-60, *Acoustic Directivity Patterns for Army Weapons.* Two concentric rings of sensors were used for the Fort Sill measurements. These sensors were placed around the central location where the weapons were fired and test charges of C-4 set off. Figure 13 illustrates the test setup. The inner ring had a radius of 250 m and the outer ring had a radius of 500 m. (Because of safety considerations, measurement stations could not be located at the full circumference of the outer ring, since part of this ring included the impact areas in front of the weapons.)

For purposes of developing the conversion factor, this chapter will compare the 500 m data gathered at Fort Sill with the 2000 ft (610 m) data gathered at Fort Leonard Wood. The difference of 200 ft (61 m) is accounted for on a 7 dB per doubling of distance basis as about 1 dB. Since the measurements at Fort Sill only occurred between about 9 AM to 4 PM, only data gathered at Fort Leonard Wood after 9 AM were used. Also, one day's data at Fort Leonard Wood, a day on which extreme wind shears occurred and anomalous propagation conditions ensued, are excluded from the data base.

At Fort Leonard Wood, measurements were made in four perpendicular directions. The data from these four directions in the appropriate time bands have been averaged together on an energy basis to develop a total average CSEL of 108.8 dB. However, Fort Sill measurements did not completely encircle the blast site -- Figure 14 shows that stations 13, 14, and 15 have no mirror image counterpart when reflected through the firing point. Fortunately, the weapons at Fort Sill were fired to the west during a period when the wind was primarily from the south to the north, allowing good average values to be developed.

To test the sensitivity of the average value developed for the Fort Sill data to various combinational schemes, five different methods were chosen to determine the average CSEL for the outer ring. In the first method, data from stations 6, 7, 8, 10, 11, 12, 13, 14, and 15 were averaged together. In the second method, data from stations 6, 7, 10, 12, and 14 were averaged together to approximate equal locations about the gun. (Station 14 data were counted twice to approximate its missing counterpart across the ring.) In the third method, data from stations 11, 8, 13, and 15 were averaged. (Station 13 and 15 data were counted twice to approximate their counterparts across the ring.) In the fourth method, data from stations 8, 11, and 14 were averaged together with the average of stations 11 and 8. (The average of stations 11 and 8 was meant to approximate the missing station opposite station 14.) In the fifth method, stations 6, 10, 12, 7, and 14 were averaged with the average of stations 6 and 10. (The average of stations 6 and 10 was used to approximate station 14.) The results of these five averaging methods are listed symbolically in Table 9.

Table 9 shows that the various methods of calculating the average around the outer ring all yield about the same results; i.e., the decibel average of the five different methods is 112.9 dB. Thus, the raw results from Fort Sill are 4.1 dB larger than the results from Fort Leonard Wood. However, as pointed out above, the measurement distance at Fort Sill was 1800 ft (500 m) instead of the 2000 ft (610 m) used at Fort Leonard Wood. Thus, the Fort Sill data as measured are about 1 dB larger than they would be at 2000 ft (610 m). Thus, the decibel factor which results from placing the C-4 charge above ground level rather than at ground level (on ground heavily pulverized by explosives) contributes 3.1 dB to the received CSEL.*

* The difference in the flat-weighted sound-exposure level (FSEL) between the Fort Sill and Fort Leonard Wood measurements was also calculated. This difference was approximately 4.7 or 3.7 dB after the distance factor of 1 dB is taken into account. The half-decibel difference between the flat-weighted factor and the C-weighted factor is accounted for by the spectral shift towards slightly lower frequencies caused by the bigger amplitudes achieved by placing the C-4 above ground level.

6 WEAPON DIRECTIVITY PATTERNS

Consideration has been given in the preceding chapters to the statistical propagation of blasts in the atmosphere. All these data are based on 5-lb charges of C-4 plastic explosive set off either above or at ground level. However, in any real military situation, a variety of charge sizes may be set off under a variety of conditions. Explosives contained in the projectile fired by artillery or armor can be thought of as various size explosives set off at or above ground level. Explosives used to propel the projectile may be any size. Further, partial containment of the propelling explosives within the gun or howitzer can both alter the magnitude of impulse produced and cause a departure from omnidirectional characteristics.

CERL TR N-60 contains all the data required to perform these translations from a 5-lb charge of C-4 plastic explosive set off on a 3-ft (0.5 m) post to any charge in a weapon. As indicated in Chapter 5, the directivity pattern and charge weight relations for the various major Army weapons were studied by performing simultaneous measures on two concentric rings at radial distances of 250 and 500 m. CERL TR N-60 contains the directivity patterns of the various weapons in relative terms (referenced to the rear of the gun). Figure 15 is a typical figure taken from that report.

Given the directivity pattern, it is necessary to translate the weight of the charge and weapon to the standard 5-lb charge of C-4 plastic explosive set off above ground level. Figure 16 graphically shows the CSEL as a function of charge weight for major Army weapons and for C-4 charges set off above ground level. Note that as the C-4 charges get substantially larger than 5 lb, the C-weighting begins to attenuate the energy, thereby causing a departure from what is otherwise a straight line. This departure from a straight line is not really evident in weapon curves, since containment of the charges by the weapon apparently precludes the frequency shift from occurring at sufficiently low frequencies.

As one final test of the developed data, it is interesting to compare the growth function vs weight relations for the C-4 charges to a theoretical prediction performed at an earlier time based on the following hypotheses:

1. The peak of the waveform grows at 2.4 dB per doubling of weight.
2. The basic spectral shift in a blast waveform is one-third-octave per doubling of weight.*

Figure 17 shows the result of the theoretical curves when C-weighting is applied compared to the results measured at Fort Sill. In this figure, both sets of data are shown relative to 0 dB for a 5-lb charge of C-4 plastic explosive. For the theoretical calculations, the relative overall composite spectrum listed in CERL TR N-13 for all stations and for all times and conditions was used.

* The 2.4 dB peak increase per doubling of weight is based on material in CERL TR I-17. The one-third-octave spectral shift per doubling of weight is based on 1975 measurements tests at Fort Leonard Wood designed to evaluate various instrumentation systems.

Table 9
Results of CSEL Averaging Methods

Method	Stations Averaged (Method)	Result (SEL)
1	$10 + 11 + 12 + 13 + 14 + 15 + 6 + 7 + 8$	112.9
2	$10 + 12 + 6 + 7 + 2 \times 14$	112.6
3	$11 + 8 + 2 \times 13 + 2 \times 15$	113.4
4	$11 + 8 + 14 + \frac{11 + 8}{2}$	112.9
5	$10 + 6 + 12 + 7 + 14 + \frac{10 + 6}{2}$	112.6

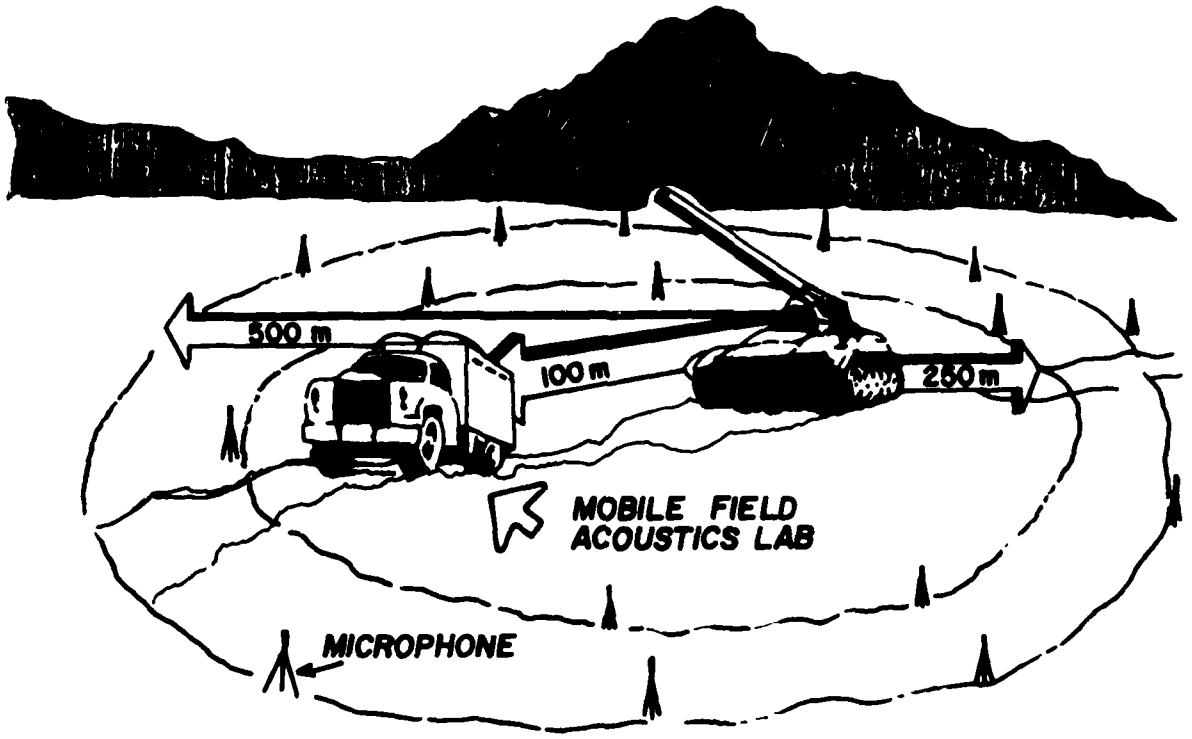

Figure 13. Location of measurement microphones for Fort Sill tests.

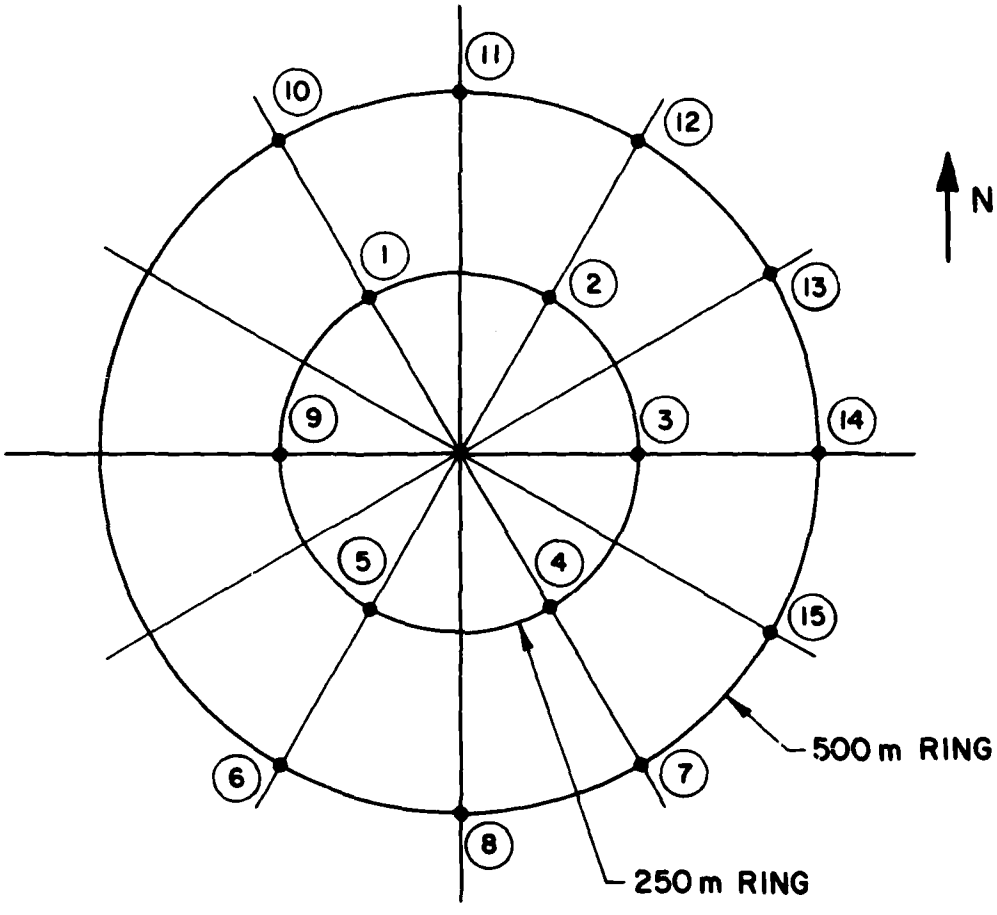

Figure 14. Position of stations 13, 14, and 15 during Fort Sill measurements.

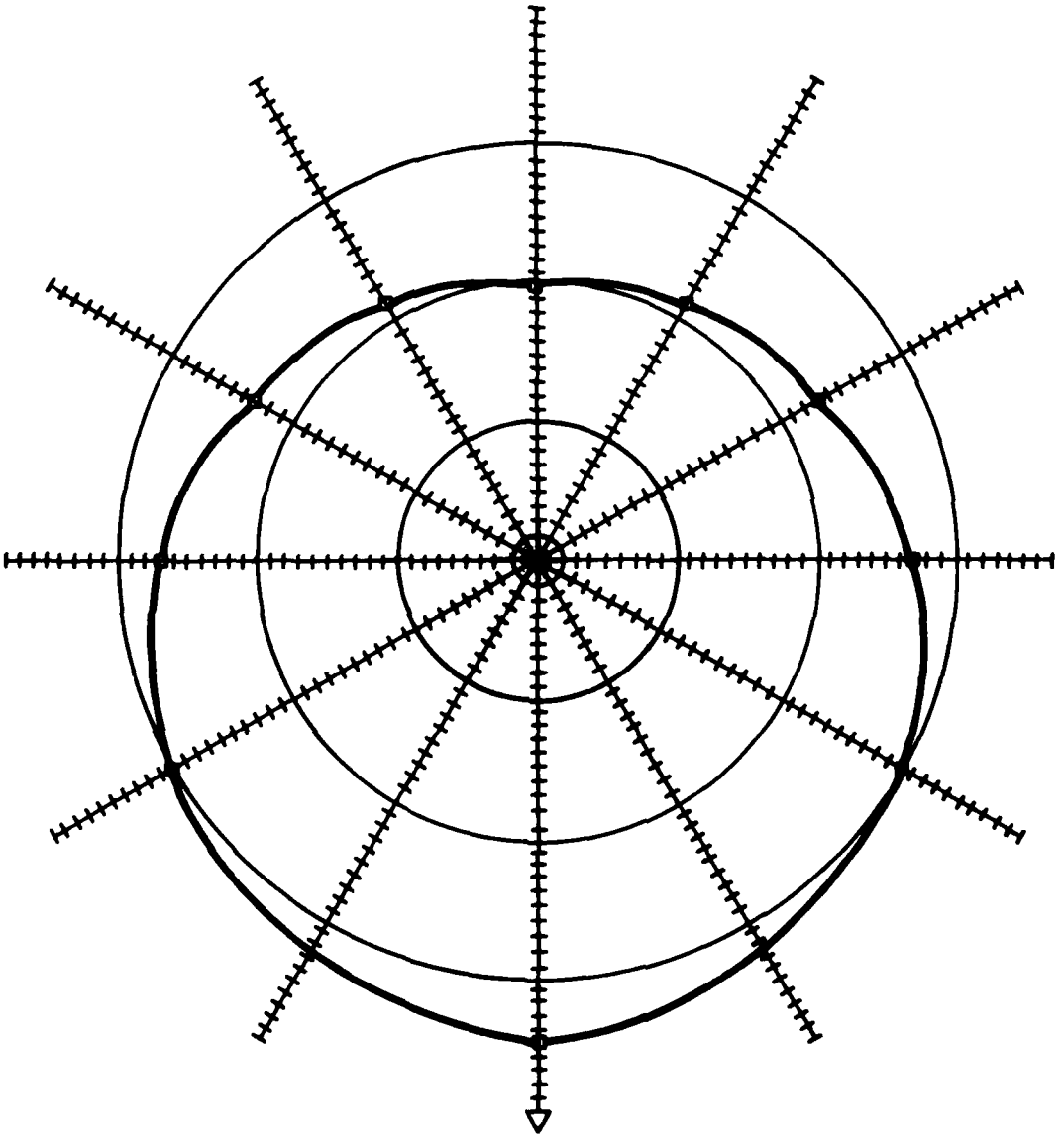

Figure 15. Directivity pattern of a towed 155-mm Howitzer.

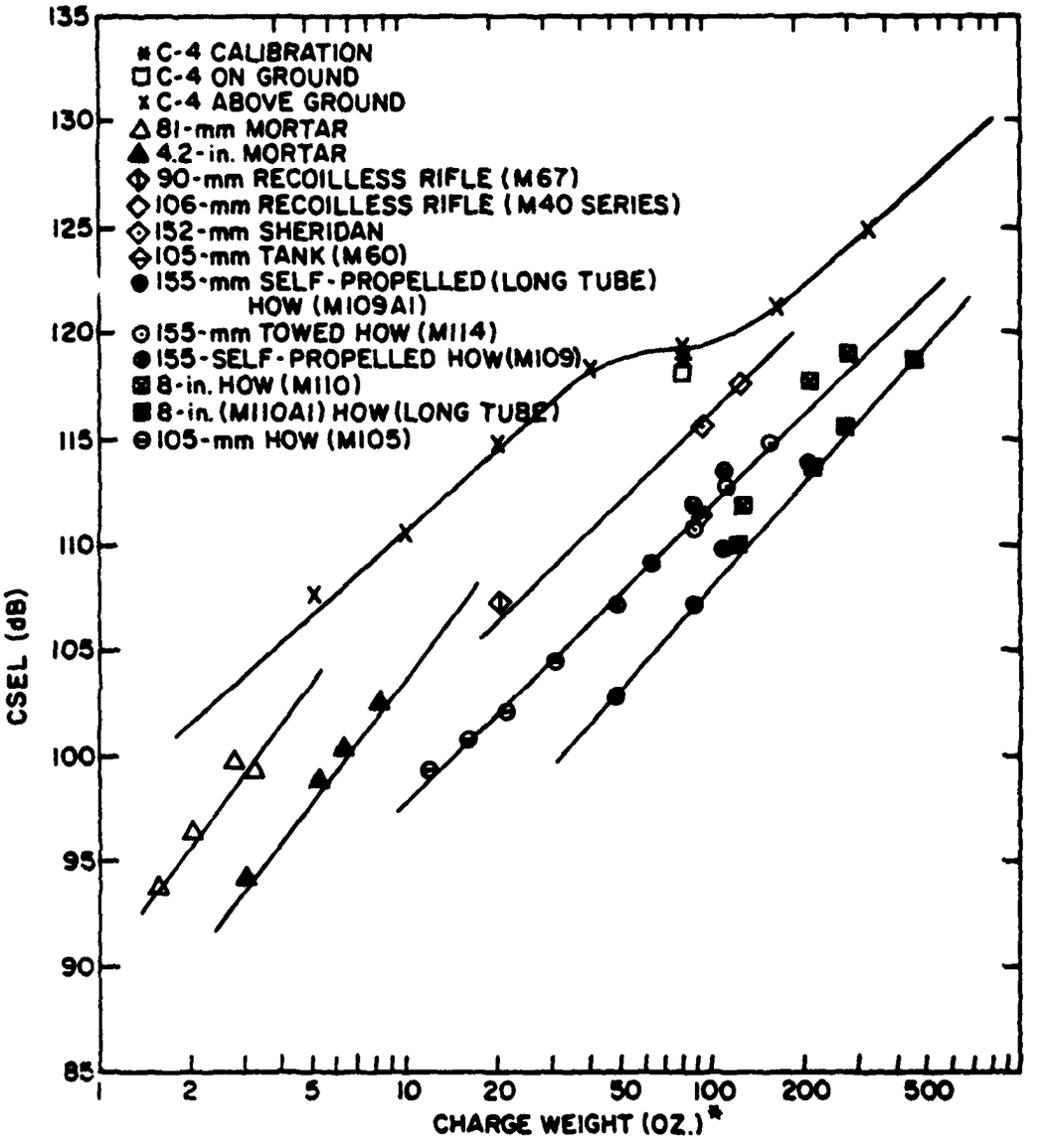

*CHARGE WEIGHT IS THE WEIGHT OF EXPLOSIVE OR PROPELLING CHARGE. THERE HAS BEEN NO CORRECTION FOR EXPLOSIVE TYPE.

Figure 16. CSEL vs C-4 charge weight.

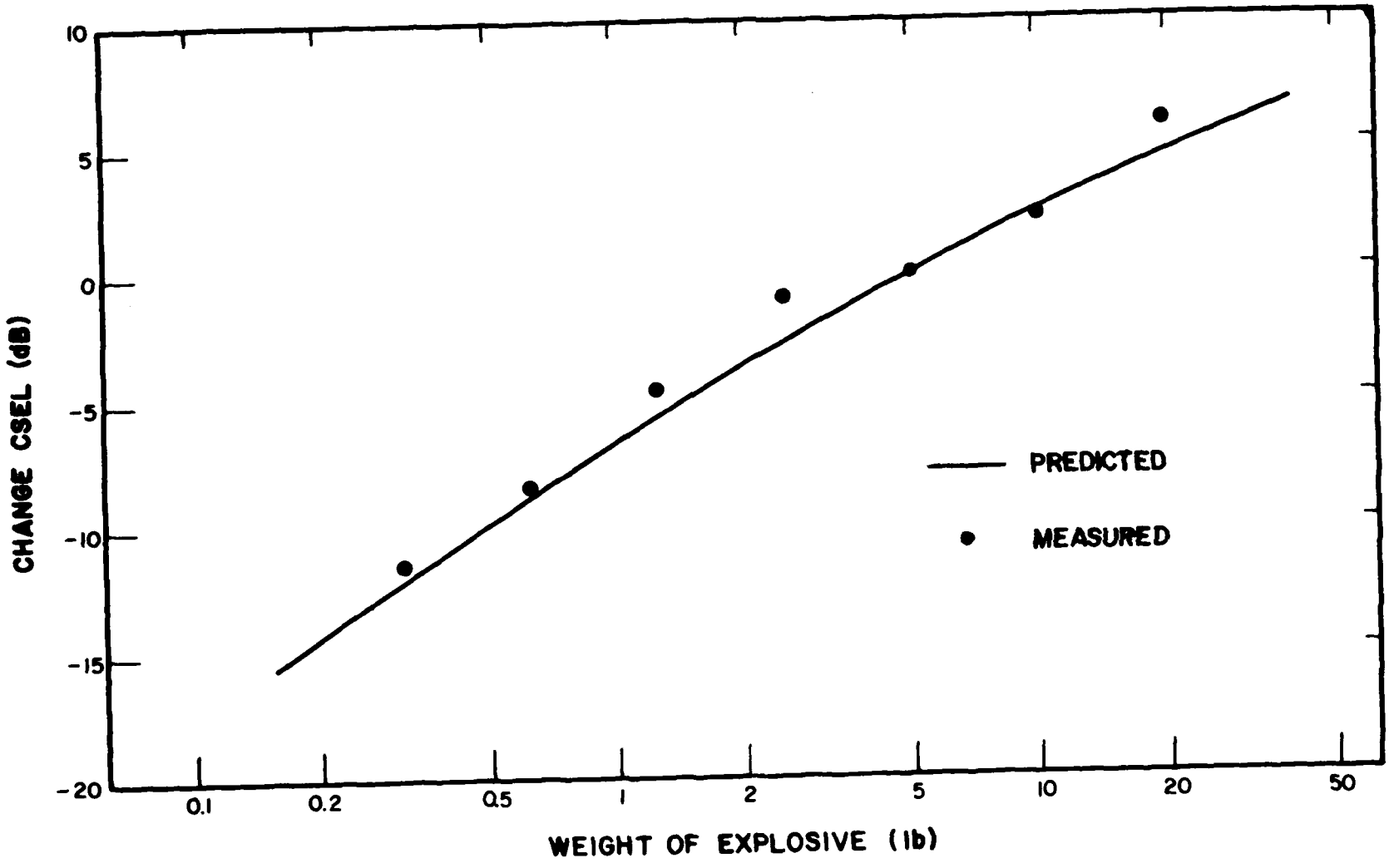

Figure 17. Predicted and measured CSEL correction factors vs weight of explosive.

7 CONCLUSIONS

This report developed or summarized the following physical data bases and computational procedures. Data bases used in the Blast Noise Prediction computer program are:

1. CSEL amplitude statistics vs distance curves for a 5-lb charge of C-4 plastic explosive set off at ground level.

2. The translation of ground level data to data gathered during tests which set off the 5-lb charge of C-4 plastic explosive 3 ft (0.9 m) above ground level, i.e., 3.1 dB.

3. The directivity patterns for the Army's major weapons.

4. The charge weight growth functions of the various weapons and explosives.

The computational procedures are:

1. Equations to translate the blast propagation statistics from the Fort Leonard Wood data base to other geographic locations and other seasons.

2. The algebraic equations and procedures to implement an arbitrary cut off or threshold within the computer calculation procedures.

APPENDIX A:

MEASUREMENT AND REDUCTION OF CLOSE-IN DATA AT FORT LEONARD WOOD

This appendix describes specific procedures used to gather close-in data from unmanned sensing stations during blast noise measurement at Fort Leonard Wood.[6]

Each unmanned sensing station consisted of a 1/2-in. 4134 B&K microphone set on top of a 4-ft (1.2-m) tripod and connected via a B&K 2619 emitter follower into a B&K 141 field measurement amplifier. The data signal from the measurement amplifier was transmitted back to the central measurement van via twisted pair lines.

The central measurement van instrumentation included Neff operational amplifiers used as line receivers and gain adjustors before recording on an Ampex FR1300 14-channel FM recorder. The gain of the 141 field amplifiers was controlled remotely in the central measurement van via a second set of lines to each station.

Calibration was performed several times a day using B&K 4220 precision acoustic ("pistonphone") calibrators. This calibration signal was recorded on the magnetic tape.

Data were reduced by playing back the recorded data into a storage oscilloscope and into the CERL-developed True Integrating Environmental Noise Monitor and Sound-Exposure Level Meter. The oscilloscope was used to view each blast individually and to separately read the positive-going peak, the negative-going peak, and the peak-to-peak amplitude. By this checking procedure, the quality and validity of these data were better ensured.

During the data reduction, a digital delay line was used in-between the FM recorder and the CERL noise monitor. This delay line triggered the monitor so that it only included in the exposure measure that period of time associated directly with an individual event. Special timing equipment enabled the CERL monitor to also sample the overall background noise level (electrical plus acoustical) associated with each event. When the monitor was interfaced with the WANG computing calculator, it was possible to automatically correct each event for the background noise level and to flag any events which were too close to the background noise level. The CERL monitor was used to develop both FSEL and CSEL data.

These data -- peak levels, FSELs, and CSELs -- were then installed in a computer for further analysis; this analysis included the histograms in Appendix B. The computerized data base was also used to develop the ground level blast amplitude correction factor.

[6] P. D. Schomer, R. J. Goff, and L. M. Little, *The Statistics of Amplitude and Spectrum of Blasts Propagated in the Atmosphere*, Volumes I and II, TR N-13/ADA033361 and ADA033640 (CERL, November 1976).

APPENDIX B:

AMPLITUDE DISTRIBUTIONS

Data collected from the close-in stations at Fort Leonard Wood were divided into two categories: (1) data which were good, clean signals and could be analyzed by the CERL monitor, and (2) data corrupted by extraneous noise or otherwise unreducible. The following distributions are based only on the data described in (1) above.

CSEL distributions were created based on the three distances: 1000 and 2000 ft (305 and 610 m) and 1 mile (2 km); and two time periods: 0500 to 0700 hours and 0700 to 1100 hours. As was previously done in CERL TR N-13 and explained for the far-out distances, the 0700 to 1600 hour histograms were given a one-fourth weighting and the 0700 to 0900 histograms were given a three-fourths weighting to better approximate a typical day's weather conditions. Figures B1 through B6 illustrate these six distributions. As these figures show, each distribution could be divided into two or more ranges using one or more natural breaks. Table B1 lists the initial and adjusted final breakpoint values which are indicated in the figures by arrows and dashed vertical lines, respectively.

Table B1
Extent of Ranges (dB)

Time Period	Distances ft (m)	Range 1* ExN	Range 2* N	Range 3* B	Range 4* F
0700 to 0500 hours	1000 (305)	--	106-118	119-125	--
	2000 (610)	50-96	97-108	109-119	--
	5280 (1640)	50-83	84-95	96-109	110-135
0700 to 1100 hours	1000 (305)	50-104	105-118	119-118	--
	2000 (610)	50-96	97-109	110-120	--
	5280 (1640)	50-87	88-98	99-108	109-135

*Range headings refer to sound velocity profile:
ExN = Excess negative
N = Negative
B = Base
F = Focus

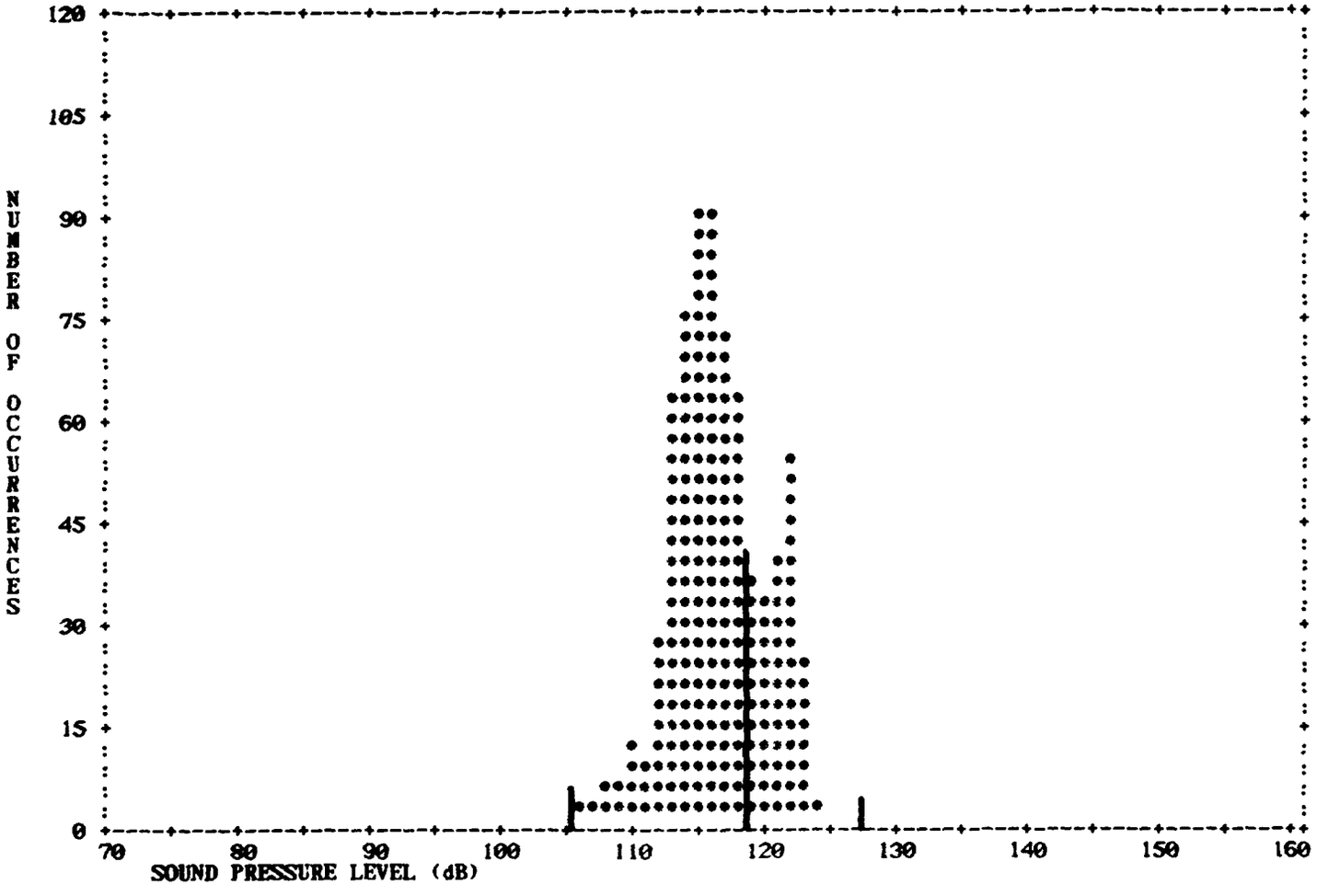

Figure B1. 1000-ft nighttime sound-pressure level distribution.

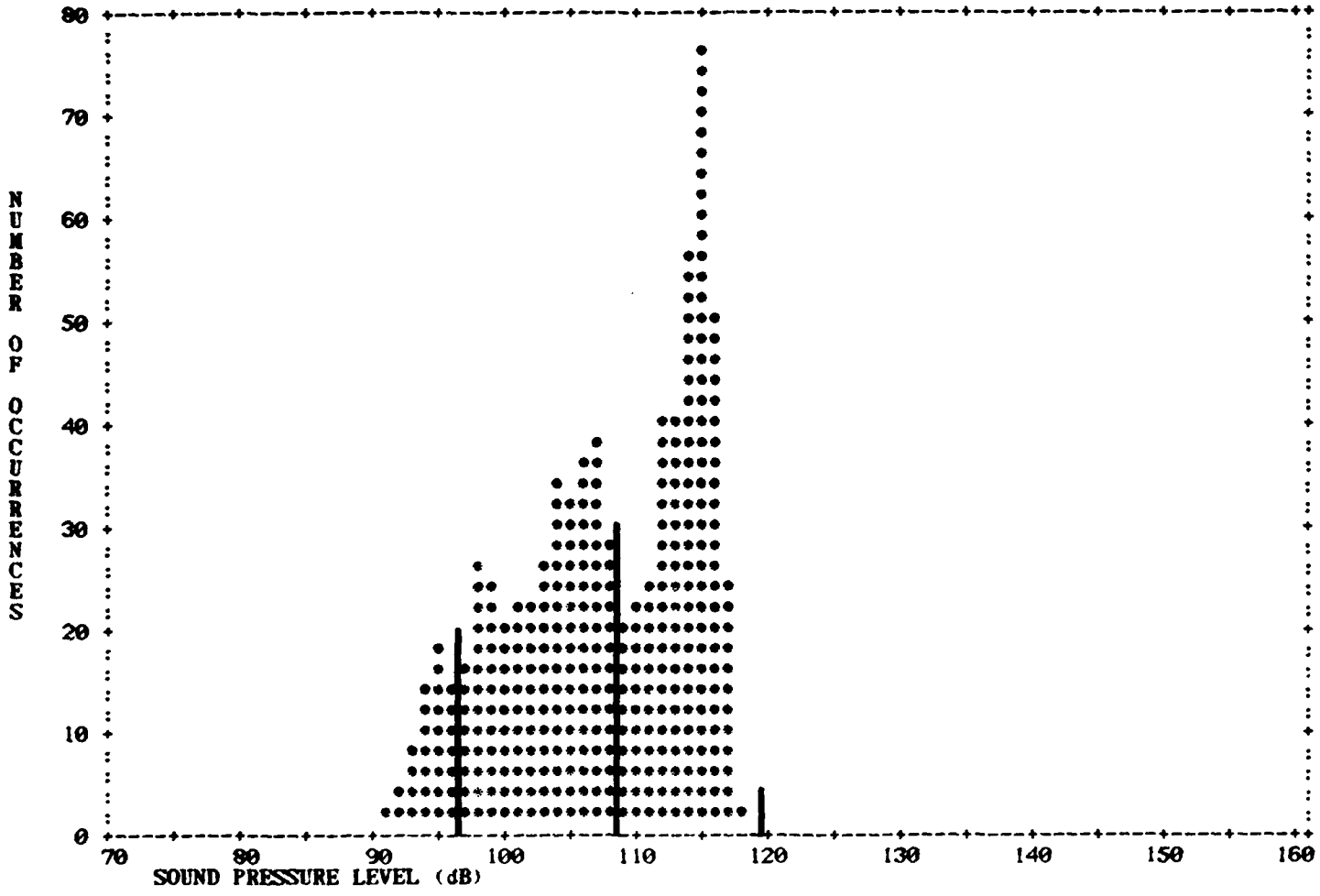

Figure B2. 2000-ft nighttime sound-pressure level distribution.

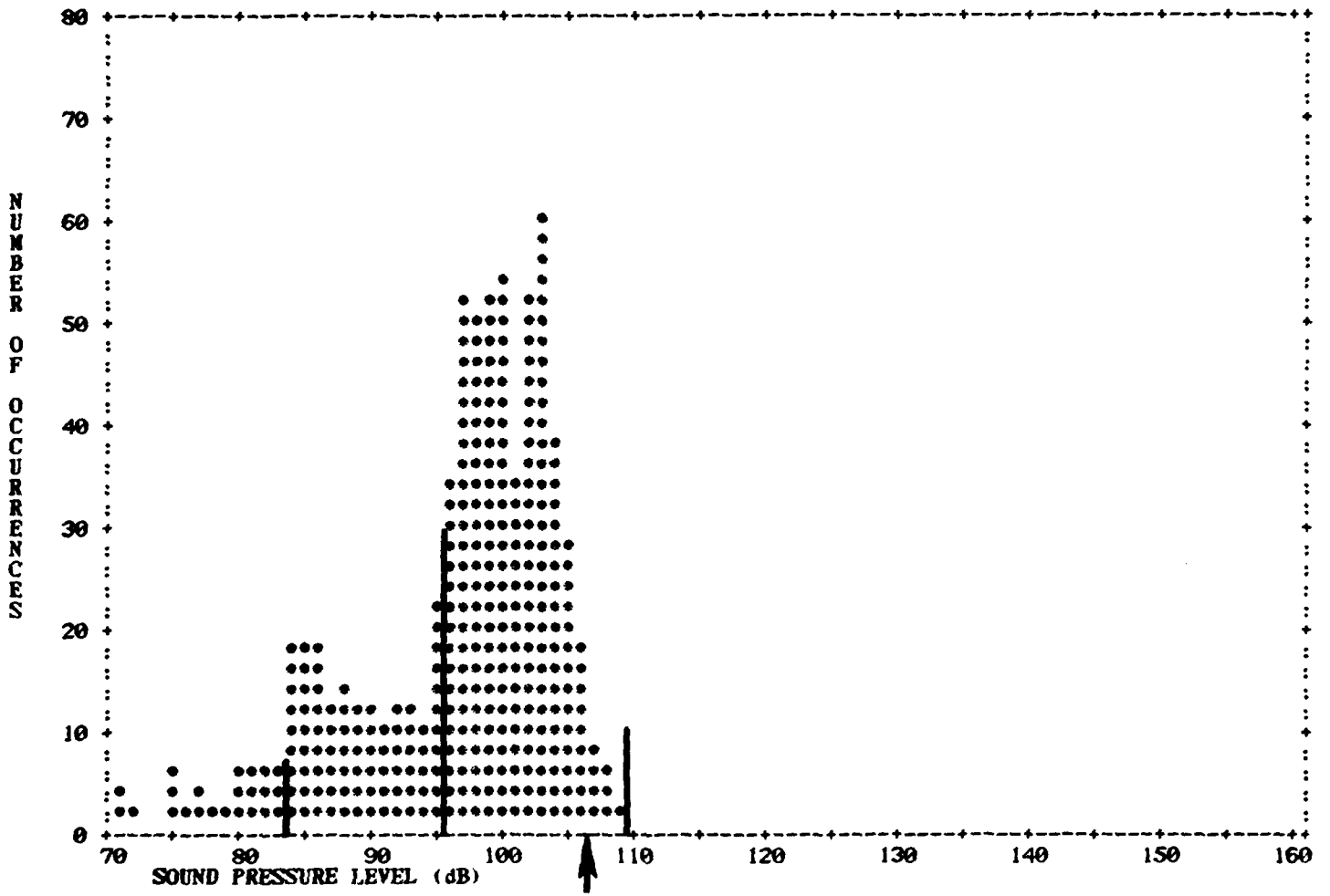

Figure B3. 1 mile nighttime sound-pressure level distribution.

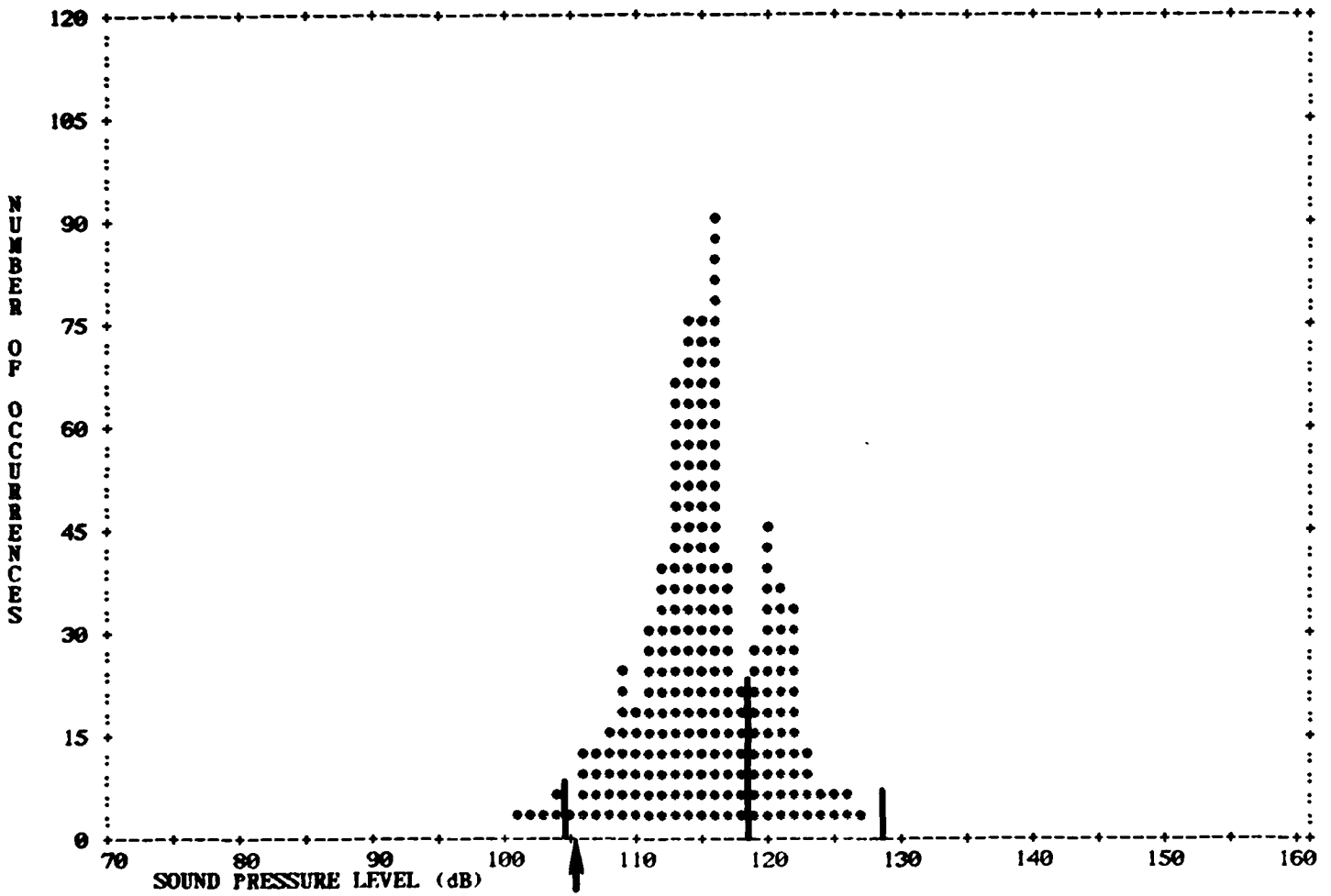

Figure B4. 1000-ft daytime sound-pressure level distribution.

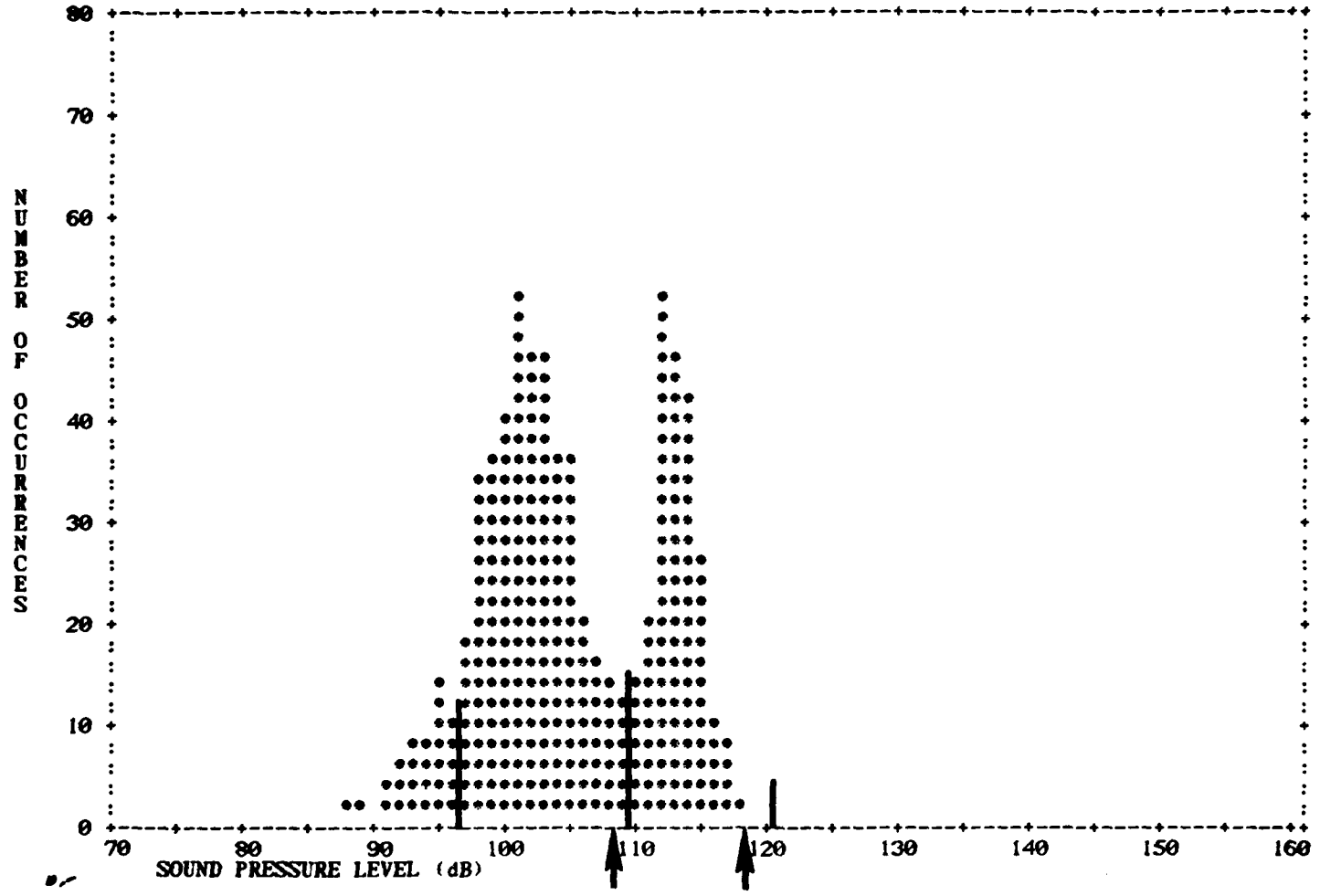

Figure B5. 2000-ft daytime sound-pressure level distribution.

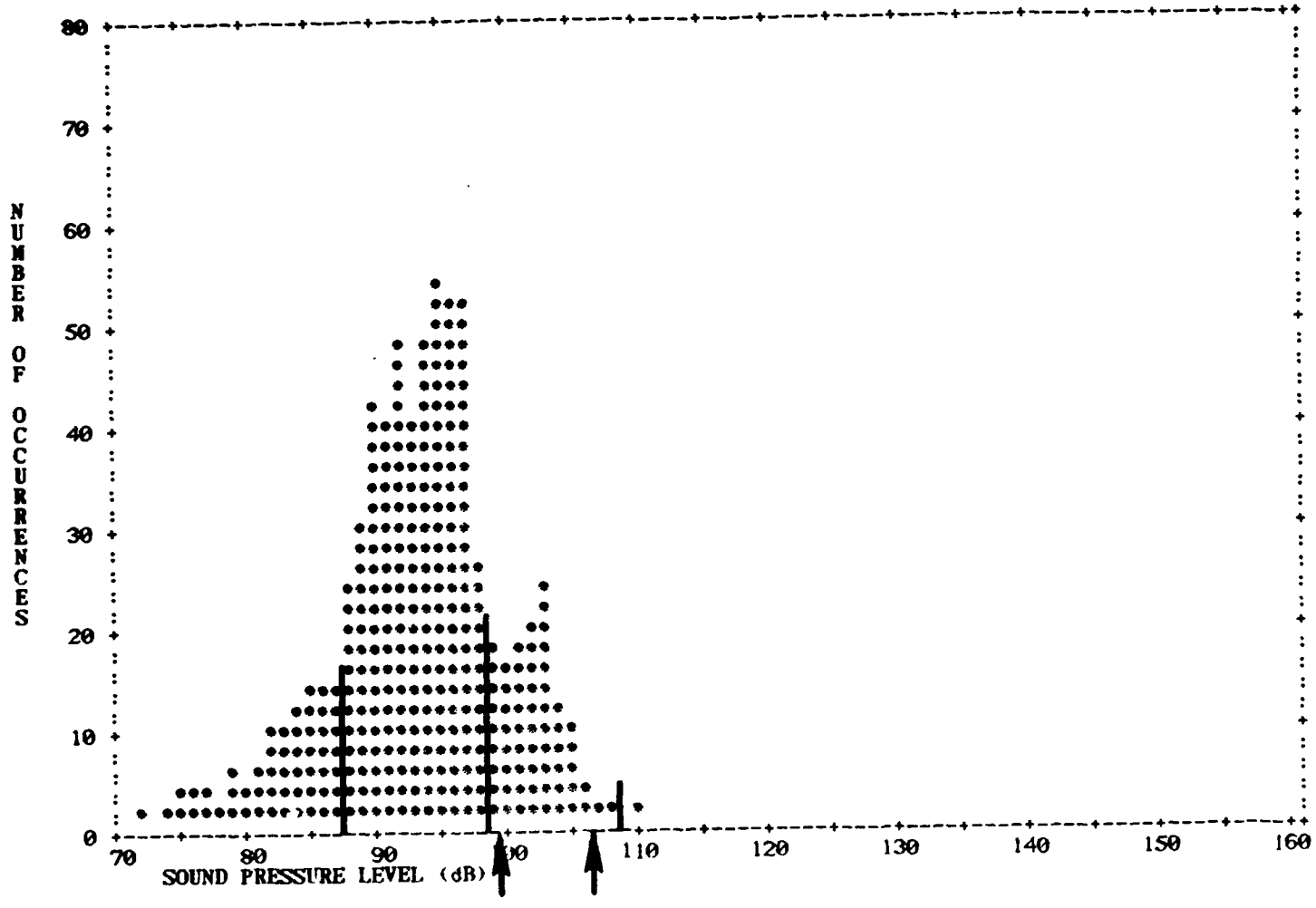

Figure B6. 1 mile daytime sound-pressure level distribution.

APPENDIX C:

EFFECT OF DISTANCE, WIND DIRECTION, AND TIME OF DAY

Figure C1 illustrates relationships between surface wind direction, time of day, and distance.* In this figure, the data are divided into 144 cells based on the following categories:

1. Four basic sound velocity profile categories (double negative, double positive, positive-negative, and negative-positive gradient)
2. Three time periods (0500 to 0700 hours, 0700 to 0900 hours, and 0900 to 1100 hours)
3. Four distances (2, 5, 10, and 15 miles [3, 8, 16, and 24 km])
4. Three wind directions (downwind, crosswind, and upwind).

The number of blast measurements and the energy average levels were entered in each cell; the cells were then aggregated into 16 larger groups based on the four sound velocity profiles and the four distances. Within each group, each of the three time periods were examined; if one wind directive was significantly larger than the others, it was marked with a square for downwind locations and a circle for upwind locations. (No crosswind locations were found to have the highest level.)

This analysis revealed that at the shorter distances and at later hours in the day, the downwind stations recorded the highest amplitude levels. At greater distances and at earlier hours of the day, the upwind stations recorded the highest amplitude levels. This was a rather unexpected result, since it is contrary to results given in the literature; however, earlier studies did not measure noise in the early morning hours. The fact that downwind stations do not always or necessarily experience the highest noise levels is quite significant in predicting both noise levels and community response.

* Blast data from categories 1 through 4 were considered for this analysis. However, since only directions within ± degrees of crosswind, downwind, or upwind were used to increase the chance of finding a significant relationship, the actual number of measurements was limited to 6739.

DISTANCE

CATEGORY		TIME*	2 miles (1.6 km) Wind Direction From	Cross	Toward	5 miles (8.0 km) Wind Direction From	Cross	Toward	10 miles (16.1 km) Wind Direction From	Cross	Toward	15 miles (24.1 km) Wind Direction From	Cross	Toward
C	NN	1	109.8	109.4	110.0	92.5	97.0	(102.7)		82.7	(103.9)		92.5	80.8
			4	51	24	8	47	29	0	19	31	0	17	9
		2	[109.7]	103.0	95.1	[98.9]	88.3	81.7	[94.0]	90.6	80.7	73.1	89.8	
			35	82	14	36	71	3	28	40	3	7	15	0
		3	[106.6]	103.8	94.0	[95.6]	87.5	73.4	88.4	95.6	92.0	80.0	86.7	
			24	85	49	25	84	19	16	32	1	2	23	0
A	PP	1	[108.7]	106.4	92.9	92.7	93.4	(106.0)	92.0	85.8	(95.8)	83.7	90.0	80.5
			69	98	18	67	129	39	13	52	39	3	26	2
T		2	[111.8]	106.9	93.8	100.2	100.1	91.1	87.9	91.5	(98.9)	83.9	91.3	89.4
			70	115	28	65	99	59	30	78	47	17	72	15
E		3	[110.9]	101.4	95.5	[101.9]	90.2	83.1	91.5	91.5	(101.0)	87.8	87.0	90.8
			53	68	29	46	43	23	33	59	6	20	26	4
G	PN	1	111.9	117.1	117.0	100.1	88.5	98.5	77.7	81.4	(86.6)	79.5		(88.9)
			45	41	2	71	71	22	26	27	24	22	0	14
O		2	[113.4]	110.4	101.5	98.4	100.8	82.5	87.8	97.4	95.0	70.6	92.7	87.5
			7	43	2	26	43	6	4	39	4	5	29	2
		3	107.2	107.4	96.8	[102.7]	90.7	77.6	[92.1]	87.6	83.2	87.4	87.0	
			47	55	13	35	44	18	32	23	13	14	12	0
R	NP	1		105.2	99.8		103.8	95.3		89.9	(98.2)		85.0	(93.8)
			0	12	28	0	1	25	0	11	33	0	1	30
Y		2	[107.3]	102.3	92.6	[109.5]	96.3	87.4	92.9	92.2	95.9	80.0	91.5	(98.9)
			6	23	27	6	19	19	7	12	10	2	6	11
		3	[107.6]	100.3	87.4	[103.3]	87.2	72.4	93.7	89.1	93.2	82.0	85.4	87.0
			7	46	5	6	24	9	6	37	5	1	11	1

*1=0500-0700 hr
2=0701-0900 hr
3=0901-1130 hr

Figure C1. Peak sound-pressure level dependence on surface wind direction, time of day, and distance.

APPENDIX D:

A METHOD WHICH FORECASTS SEASONAL OMNIDIRECTIONAL SOUND-EXPOSURE LEVELS USING METEOROLOGICAL CONDITIONS

The studies cited in this appendix have examined sound propagation in the atmosphere and reported the phenomenon of focused acoustical energy at large distances from sound sources.

General

Impulse noise from explosions provides a measurable quantity for testing and also represents a type of acoustical energy which is liable to cause structural damage to buildings and an extreme nuisance to the population. The goal of research groups such as the Ballistics Research Laboratories and Sandia Laboratories has been to develop procedures which can predict sound propagation paths and possible focused energy in specific blast-by-blast conditions. Most of these studies include all parameters that could affect acoustic wave propagation including (1) directionality of blast source, (2) height of source with respect to ground, (3) terrain types, (4) vegetation, (5) humidity, (6) low-level air turbulence, (7) temperature gradients, and (8) wind. The theoretical results of these studies generally agree.[7] The parameters which these studies indicate play the major role in determining sound propagation paths are temperature gradients, wind, and major terrain variations.

This appendix applies temperature and wind parameters to develop a method of defining total energy curves in four directions for any geographic location. These total energy curves exhibit the amount of energy that will occur at a particular distance away from the source over whatever period of time is desired, e.g., a season. The total energy represents the summation of all the types of energy that are directed to specific locations and is representative of the type of weather conditions that occurred most often during the test periods.

Terrain effects are not considered, since there is currently no way to define how physical characteristics such as large land forms and water bodies alter sound propagation paths.

The method described in this appendix is defined by comparing meteorological data with impulse noise data taken simultaneously during tests performed in June 1973 at Fort Leonard Wood.

Theory

The prediction of sound propagation paths requires a thorough understanding of not only acoustic wave theory, but also the effects of atmospheric structure on certain properties of the acoustical wave. Using an explosion as a noise source is theoretically equivalent to a spherical source mounted in an infinite baffle, which will radiate a hemispherical sound wave until atmospheric and terrain characteristics alter the propagation.

A strong explosion will initially exhibit the classical pressure-time signature shown in Figure D1, which consists of a sharp compression followed by a gradual pressure decay into a rounded negative-pressure phase and gradual recovery. This blast wave attenuates very rapidly into a sound wave (the terms "blast wave" and "sound wave" will be used synonomously in this appendix).

Using a simple atmosphere model in which temperature is constant with ascending altitude and wind is not present, the sound wave travels away from the source in a hemispherical fashion. If specific sound ray paths were drawn for this model, the picture would be similar to spokes around the hub of a wheel (Figure D2; this figure also shows the associated sound velocity profile of zero gradient). The diagram showing the ray paths in Figure D2 is called "ray tracing," and will be used to designate other

[7] B. Perkins, Jr., P. H. Lorrain, and W. H. Townsand, *Forecasting the Focus of Air Blast Due To Meteorological Conditions in the Lower Atmosphere*, Report No. 1118 (Ballistics Research Laboratories, 1970); B. Perkins, Jr. and W. F. Jackson, *Handbook for Prediction of Air Blast Focusing*, Report 1240 (Ballistics Research Laboratories, 1964; and J. W. Reed, *Acoustic Wave Effects Project: Airblast Prediction Techniques*, SC-M-69-332 (Sandia Laboratories, May 1969).

types of gradients later in this appendix. Note that the sound ray paths merely represent the direction of travel of a sound wave front.

The ray tracing in Figure D2 is based on the fact that there are no parameters affecting the acoustic properties. Therefore, the sound speed is constant everywhere. It has been shown that in this simple atmosphere model, the amplitude of sound is inversely proportional to the distance from the source.[8] Thus, energy density is inversely proportional to the square of distance. This represents the normal rule of thumb for sound pressure level (SPL); i.e., SPL decreases by 6 dB each time distance is doubled. This incremental SPL decrease is the normal attenuation to be expected with lateral distance. If an energy density curve defines the SPL as declining by less than 6 dB per doubling of distance, it is assumed that the sound energy was reinforced at the particular distances by some interaction with the atmosphere.

When sound energy is reinforced, sound ray paths become reflected and refracted in the atmosphere in a way similar to the effect of a lens or prism on light. Researchers such as Reed, Perkins, and Thompson, have explained that the variation of sound velocity with altitude causes the bending of sound ray paths.[9] Variation of sound velocity with altitude is dependent on temperature and wind changes with rising altitude and can be represented by sound velocity profiles where the sound velocity (in m/s) is represented by:

$$SV = 331.6\sqrt{1 + T/273} + \textit{wind component} \qquad \text{[Eq D1]}$$

where T is the temperature in degrees centigrade.

As a general rule, wind speed increases and temperature decreases with ascending altitude. This simple rule is usually visualized in a sound velocity profile as a negative gradient. The negative gradient profile and its ray tracing can be seen in Figure D3. Note that the sound ray path in Figure D3 is bent upward, creating greater than normal attenuation with lateral distance.

Temperature or wind speed increases with altitude cause the sound velocity profile to have a positive gradient. A simple positive gradient profile along with its ray tracing is seen in Figure D4. A positive gradient causes amplification of sound energy by bending the sound ray paths back to the surface. The types of sound velocity profiles that produce sound-energy focusing are those that have a drastic change in slope at some altitude above the surface. Methods of ray tracing have been explained by Perkins and Thompson.[10]

Because it is very rare for the atmosphere to be completely stable, the conditions for alteration of sound ray paths are always present. The problem becomes one of determining where sound energy could focus under a given sound velocity profile. The sound velocity profile is, in turn, dependent on weather conditions. Therefore, a discussion of weather and its diurnal variations is necessary.

Diurnal variations in meteorological elements are caused primarily by the sun heating the temperature of air. For example, surface winds are created when air flows toward the area of highest heating. The speed of surface winds increases gradually from sunrise to approximately mid-afternoon, when the maximum air temperature is reached. However, as the heating effects of the sun decline during the late afternoon to just after sunset, the wind speed rapidly falls. Wind speed declines only slightly during the rest of the night. Of course, the surface wind speed rarely approaches the magnitude of high-altitude air movement, which can be considered almost constant for short-term studies.

When considering temperature variations, the ground becomes another important parameter. During the day, the earth acts as a bank of heat, absorbing the sun's energy. The air near the surface is then heated by conduction from the ground.

---

[8] L. L. Beranek, *Noise Reduction* (McGraw-Hill, 1960).

[9] J. W. Reed, *Acoustic Wave Effects Project: Airblast Prediction Techniques*, SC-M-69-332 (Sandia Laboratories, May 1969); B. Perkins Jr., et al., *Forecasting the Focus of Air Blast Due To Meteorological Conditions in the Lower Atmosphere*, Report No. 1118 (Ballistics Research Laboratories, 1960); R. J. Thompson, *Sound Rays in the Atmosphere*, SC-RR-64-1756 (Sandia Laboratories, January 1965); and R. J. Thompson, *Computing Sound Ray Paths in the Presence of Wind*, SC-RR-67-53 (Sandia Laboratories, February 1967).

[10] B. Perkins, Jr., P. H. Lorrain, and W. H. Townsand, *Forecasting the Focus of Air Blast Due to Meteorological Conditions in the Lower Atmosphere*, Report No. 1118 (Ballistics Research Laboratories, 1960); R. J. Thompson, *Sound Rays in the Atmosphere*, SC-RR-64-1756 (Sandia Laboratories, January 1965).

At night, the earth's outgoing radiation exceeds the incoming. Therefore, the surface loses the heat it gained during the day and subsequently cools. As the temperature declines at the surface, the air near the surface is cooled by conducting its heat to the ground. When this occurs, temperature inversions are formed in which temperature actually increases with height. This effect tends to trap the lower air layer, which is sometimes visible as fog when condensation also occurs. When the sun rises again, the ground and air near the ground is reheated. The heated air pushes the inversion layer higher, and as the day progresses, the inversion layer is dissipated by the sun and the wind. It is important to note that this inversion layer (in some cases many inversion layers) is the prime cause of sound energy focusing.

It is also important to note that the wind can affect sound propagation paths. Sound velocity is strengthened downwind and retarded upwind; therefore, the sound velocity profile is different in each direction and must be considered when determining locations for sound energy focusing (Figure D5).

Development

To define blast noise data in an area simply by manipulating weather data, acoustical theory must be applied to the weather conditions and the impulse noise source. This will allow theoretical blast statistics to be forecast. Then, by comparing the predictor set with the actual blast data, a relation can be devised to reduce error in prediction and finalize the method of obtaining predicted blast energy curves. Because this method should be applicable at practically any geographic location and should represent seasonal means and standard deviations, not specific single-time events, certain simplifying assumptions can be made:

1. To evaluate meteorological effects, major terrain variations can be neglected.

2. The sound source is nondirectional (although the initial product of a blast is a shock wave, it quickly deteriorates into a spherical acoustical wave).

3. Only diurnal variations have to be considered, since large-scale meteorological conditions such as pressure zones and weather fronts change slowly and remain sufficiently constant for about 8 hours.

Data Compilation

The actual blast data used to derive the method described in this appendix were compiled by Schomer at Fort Leonard Wood in June 1973.[11] These tests consisted of 735 noise-monitoring trials using stations located in each of four directions 2, 5, 10, and 15 miles (3.2, 8.0, 16.1, and 24.1 km) away from the blasting site. During all tests, an FAA plane collected both temperature and wind data at various altitudes. Unfortunately, the FAA weather data could not be completely used because of instrument errors and a controversy which subsequently arose concerning the reliability of the FAA data. It was possible, though, to use weather data recorded by radiosonde methods at Monette, MO.*

To compare weather conditions with blast statistics, data over the same period of time must be used. Weather stations make their radiosonde observations only twice a day -- at 1200 Z (Greenwich Mean Time; 6 AM Central Standard Time [CST]) and 0000 Z (6 PM CST). Since the Fort Leonard Wood blast data were only collected from 5 to approximately 11 AM CST, the obvious choice of weather data was that collected at 6 AM. Therefore, if this choice of weather data is considered as the average condition for the period of 6 to 8 AM for the particular data, the blast data that should be used are those that occur within that same period.

The Fort Leonard Wood blast data were listed at each recording station in terms of the number of occurrences of each decibel level. To produce the actual total energy curves, all the data were summed on an energy basis at each station. This produced 16 energy totals -- one for each

[11] P. D. Schomer, R. J. Golff, and L. M. Little, *The Statistics of Amplitude and Spectrum of Blasts Propagated in the Atmosphere*, Volumes I and II, TR N-13/ADA003361 and ADA033646 (CERL, November 1976).

* For use in averaged calculations, manipulation of weather data not obtained directly at the blasting site is acceptable when the data collection point is reasonably near the blast site and if no major terrain changes or obstacles are between the blast site and data collection point. Therefore, it is probable that weather station data can usually be used to define blast statistics.

direction. Therefore, the weather data had to be reduced to 16 predictor numbers if it was to be related to the energy data.

Weather Data Predictors

Radiosonde weather data are listed in terms of temperature, wind speed, and wind direction at various altitudes. To develop appropriate predictors, an understanding of the physics of sound propagation is required. Previous researchers have determined that the path sound waves follow in the atmosphere is reflected and refracted.[12] This path is dependent on the shape, magnitudes of gradients, and altitudes of the base, or top of inversions, of the sound velocity profile. The sound velocity (in m/s) at each altitude can be calculated by the following relation:

$$SV = 331.6(1 + T/273)^{1/2} + DW \qquad \text{[Eq D2]}$$

where T is the temperature in degrees centigrade, DW is the wind component in the direction under investigation, and SV is sound velocity.

The Ballistic Research Laboratories simplifies this equation to:

$$SV = (0.6096)\,T + DW \qquad \text{[Eq D3]}$$

This simplification results from the fact that sound paths are determined from changes in the sound velocity profile, rather than changes in the actual magnitudes. The sound velocity increases 0.6096 m/s for a rise in temperature of 1^{o}C. It can be seen that the sound velocity profile is affected equally in every direction by temperature structure, but that the wind component is different for different directions. Therefore, the sound velocity for each direction must be computed for each day considered and at each altitude considered. Figure D6 shows an example of how the sound velocity profile differs for each direction.

The sound velocity profiles must be categorized into standard groupings so they can be added to develop weather statistics. The most obvious categorization is the shape of the sound velocity profile. This is an important parameter because the shape of the profile determines whether focusing, amplification, normal attenuation, or silence will occur at any given distance. The five shapes that were chosen to represent all possible combinations are shown with their ray tracings in Figure D7. These shapes were also pointed out by Perkins as the most common and important shapes among those that can occur.[13] Within each category, the "mean" altitude of change and magnitudes of gradients, along with their standard deviations, are calculated after summing the sound velocity profiles (in their respective categories) for all the days during which actual blast data are collected. (It is possible to determine how often each type of profile occurs by tallying the profile categories and developing the percentage of occurrence of each type of profile.)

[12] B. Perkins, Jr., P. H. Lorrain, and W. H. Townsand, *Forecasting the Focus of Air Blast Due to Meteorological Conditions in the Lower Atmosphere*, Report No. 1118 (Ballistics Research Laboratories, 1960); B. Perkins, Jr. and W. F. Jackson, *Handbook for Prediction of Air Blast Focusing*, Report No. 1240 (Ballistics Research Laboratories, 1964); J. W. Reed, *Acoustic Wave Effects Project: Air Blast Prediction Techniques*, SC-M-69-332 (Sandia Laboratories, May 1969); T. M. Georges and S. F. Clifford, "Acoustic Sounding in a Refracting Atmosphere," *Journal of the Acoustical Society of America*, Volume 25, Number 3 (May 1953); V. Ingard, "A Review of the Influence of Meteorological Conditions on Sound Propagation," *Journal of the Acoustical Society of America*, Volume 25, Number 3 (May 1953); and E. F. Cox, H. J. Plagge, and J. W. Reed, "Meteorology Directs Where Blast Will Strike," *Bulletin of the American Meteorological Society*, Number 3 (March 1954).

[13] B. Perkins, Jr. and W. F. Jackson, *Handbook for Prediction of Air Blast Focusing*, Report No. 1240 (Ballistics Research Laboratories, 1964).

From this point, the method developed at the Ballistics Research Laboratories can be used to transform each of the five sound velocity profiles, which now represent the average profile of each category, into the set of predictors. There are two ways of using the Ballistics Research Laboratories' method. One way is to consider not only the paths of the "mean" profile but also the "mean" + "standard deviation" profile of each category. These can be thought of as developing a scatter of sound velocity profiles. This method can be computerized.

To further test the choice of predictor method, the data collected during the Fort Leonard Wood tests were used. The time period was extended to an all morning period of each day (6 to 11 AM) during the entire 3 weeks of the experiment. Weather data for the period following 8 AM were forecast based on typical diurnal variations. These forecasted weather data were used to develop an enlarged set of predictors. From these predictors, the total energy curves for 8 to 11 AM were estimated and added to the total energy curves from 6 to 8 AM to determine the predicted curves for all morning blast activities. When these predicted total energy values were compared with the actual values, a correlation of 0.90 was found. The actual and predicted total energy curves for each direction are plotted in Figures D8 through D11.

Method

The following describes a step-by-step method of predicting total energy curves representing blast propagation statistics for any location using meteorological data obtained at a weather station near that location. To provide a representative example, tables are presented which list data collected during the Fort Leonard Wood experiment.

Generally, predictions should be made for 2-hour time blocks. If a much larger period than 2 hours is required, it is suggested that (1) the energy curves for 2- to 3-hour periods be computed, and (2) energy curves of all the periods be summed to produce the total energy curves for the larger time block.

Only data taken up to an altitude of 200 m above ground level are required.

Preparing Weather Data

If weather data are not available for the particular time period desired, or if large blocks of time are required, data can be predicted from weather station data for another time by consulting diurnal variation characteristics at the given location.

Radiosonde-recorded weather data can be obtained from the nearest National Weather Station for any season desired, at 1200 and 0000 Z of each day (Table D1).

1. Weather stations list altitude data in geopotential meters above sea level. When developing these data, altitude units must be converted to meters above surface level. In the weather station listing, the ground level altitude (geopotential meters above sea level) is denoted as G. By defining the parameter M as a weather station altitude and F as the desired altitude listed in meters, the following equation can be used to produce the correct height:

$$F = (0.98)^{-1}[M-G] \qquad \text{[Eq D4]}$$

2. The wind components (in m/s) in each of four directions (North = 0^{o}, East = 90^{o}, South = 180^{o}, West = 270^{o}) for each day and for each altitude throughout the season in question are calculated by:

$$\begin{aligned} &\text{North wind } \Xi = \text{NW} = \text{W}\cos(180°-\Theta) \\ &\text{East wind } \Xi = \text{EW} = \text{W}\sin(180°-\Theta) \\ &\text{South wind } \Xi = \text{SW} = -\text{NW} \\ &\text{West wind } \Xi = \text{WW} = -\text{EW} \end{aligned} \qquad \text{[Eq D5]}$$

where W is the wind speed in meters per second and Θ is the direction of the wind listed in degrees.

3. These data can be listed in tables which include the temperature and wind date for each altitude (Table D2).

Developing Sound Propagation Statistics

1. The weather data listed in Table D2 can be completed by using the Ballistics Research Laboratories simplified sound velocity estimation, which is represented in the following relationships. Note that these values are all dependent on altitude.

$$\begin{aligned} \text{SV North} &= SV_N = 0.6096T + NW \\ \text{SV East} &= SV_E = 0.6096T + EW \\ \text{SV South} &= SV_S = 0.6096T + NW \\ \text{SV West} &= SV_W = 0.6096T + EW \end{aligned} \qquad \text{[Eq D6]}$$

2. Next, the four sound velocity columns representing the sound velocity profiles for each day must be scanned to determine (a) the shape of the profile, and (b) the appropriate gradient magnitudes and altitude levels. The five categories of sound velocity profiles are shown in Figure D7, along with the appropriate parameters that are to be distinguished. A table similar to that shown in Table D3 should be prepared for each direction, listing each occurrence of a particular profile over the season in question.

$$\% = \textit{Percent occurrence} = \frac{\textit{type total occurrence}}{\sum \textit{type total occurrence}} \qquad \text{[Eq D7]}$$

Blast Statistics Prediction

1. The heuristic approach that follows requires knowledge of sound propagation theory. Using the mean sound velocity profile data for each type of profile (e.g., Table D3) and the example cases in Ballistics Research Laboratory Report No. 1240 requires that ray tracings for each type of profile in each direction be drawn.

The ray tracings in Figure D7 can be used as a guide to assign weighting factors to the ray tracings developed from the sound velocity "mean" profiles. A weighting factor is necessary for each distance desired.

As a computational method, an electronic ray tracer can be used to produce sound propagation diagrams from the sound velocity profiles described by the means (μ) and standard deviations ($+ \sigma$) in Table D3. To make these cound velocity profiles representative, the μ, ($\mu + \sigma$), and ($\mu - \sigma$) conditions must be traced. How focal areas vary with the shape of the profile can then be observed. When considering how to assign weightings at a given distance, a bell curve is plotted around the distance at which the "mean" profile defines a focus. Then, as an approximation, the standard deviation points on the bell curve can be weighted as the mean weighting minus 1. Figure D12 is an example of the combination of μ and ($\mu + \sigma$) sound velocity profiles.

The "scaled percentage" label (Table D4) actually indicates factors which are determined from that category in which the percent of occurrence of a type of profile exists as described in Table D5.

If the distance-dependent predictor is labeled as P(d), the scaled percentage as Xi, the type weighting as Yi (where i = I, II, III, IV, V), and the distance as d, then the following equation completes the prediction method:

$$P(d) = \sum_{i=I}^{V} XiYi(d) \qquad \text{[Eq D8]}$$

where P and Yi are dependent on distance. Note that Yi represents the weighting factors which are determined by comparing the averaged sound velocity profiles with those examples in Figure D7. Figure D7 shows the type of weight to be assigned at different distances and various sound velocity types.

The predictors, P(d), are not the total energy values. An equation is needed that relates the predictor set to the actual total energy set. A suitable relation is found by forming a linear regression (the

sum of the least squared differences) between the set of predictors found and the set of actual total energy data for the Fort Leonard Wood experiment. The line of regression produces the following relation:

$$Total\ (Energy)\ SEL = 0.076P + 98.9(dB) \qquad \text{[Eq D9]}$$

where P and Total Energy are not dependent on distance. When applying a distance criterion, the normal attenuation factor must be incorporated. Then the final equation including distance dependence on the Total Energy (in decibels) becomes:

$$Total\ (Energy)\ SEL(d) = 0.76P(d) + 98.9 - 22.3 \log_{10}(d) \qquad \text{[Eq D10]}$$

The result is a Total (Energy) SEL for each distance in each direction.

Results

The results of using the method described in this appendix on the Fort Leonard Wood weather data are listed in Table D6, and are compared to the actual total energy data for the periods in question. Note that for the larger time period of 6 to 11 AM for the 3 weeks in June 1973, the predicted set was formed by adding columns 2 and 5 on an energy basis.

Graphical results for the 6 to 8 AM period are presented in Figures D8 through D11. These graphs show that the shapes of the actual and predicted curves are similar.

The validation of the accuracy of the method described in this appendix is demonstrated by the resulting correlation between the predictor set and the actual total energy values. It was found that the set of predictors had a correlation of 0.904, which states that approximately 82 percent of the variability of total energy is caused by the weather predictors selected.

Discussion

The method described in this appendix may provide an improvement over other methods used to forecast blast statistics at various geographical areas. These other procedures are based on a comparative ratio system to an example situation, whereas this method provides a direct calculation. The method described in this appendix successfully predicts the amount of sound exposure at locations surrounding a blasting site. The amount of energy defined is an average dependent on weather characteristics during the period of time in question. However, more data are required to validate this procedure.

Table D1
Example Weather Station Data

Date (month/day)	Pressure (millibars)	Level (Geopotential) (m)	T (Temperature) (°C)	Relative Humidity	θ (Wind Direction) (degrees)	W (Wind Speed) (m/s)
6/11	966.1	G = 438	19.0	0.92	170	2
	950.0	584	21.7	0.92	210	5
	949.0	593	21.9	0.89	212	6
	900.0	1053	19.4	0.82	221	11

Table D2
Example Converted Weather Data

Date (month/day)	Altitude (m) (Geopotential)	Altitude (F) (m)	Temperature (°C)	NW (m/s)	EW (m/s)	SV_N (m/s)	SV_E (m/s)	SV_S (m/s)	SV_W (m/s)
6/11	438	0	19.0	1.97	−0.35	13.55	11.23	9.61	11.93
	584	146	21.7	4.33	2.50	17.56	15.73	8.90	10.73
	593	155	21.9	5.09	3.18	18.49	16.58	8.31	10.22
	1053	615	19.4	8.30	7.22	20.13	19.05	3.53	4.61
	1544	1138	16.7	8.19	5.74	18.37	15.92	1.99	4.44
	2059	1621	13.3	8.40	3.23	16.51	11.34	−0.29	4.88
	2326	1888	11.5	8.65	2.48	15.66	9.49	−1.64	4.53
	2600	2162	9.9	9.51	3.09	15.55	9.13	−3.47	2.95

Table D3
Direction: *South*
Accumulation of Sound Velocity Profile Types

Calculated Parameter*	Type 1 g_1	Type 2 g_1	Type 2 Alt.	Type 2 g_2	Type 3 Alt.	Type 3 g_2	Type 4 g_1	Type 4 Alt.	Type 4 g_2	Type 5 g_1	Type 5 Alt.	Type 5 g_2
	−0.006	0.0114	175	−0.004			0.0063	175	0.0115	−0.0045	625	0.004
	−0.0053	0.0074	625	−0.005			0.0017	375	0.003	−0.015	625	0.003
	−0.004	0.020	175	−0.0024						−0.0195	625	0.0047
		0.044	175	−0.004						−0.0034	175	0.0058
										−0.030	175	0.006
										−0.008	625	0.007
										−0.003	375	0.0054
	μ −0.0051	0.0182	355	−0.0037			0.004	275	0.0073	−0.0119	460.7	0.0051
	σ 0.001	0.0153	246.5	0.001			0.0033	141.4	0.0060	0.0101	215.5	0.0013
	ω 3		4		0			2			7	
	% 18.75		25		0			12.5			43.75	

*μ is the column mean.
σ is the column standard deviation.
ω is the number of entries in the column.
% is calculated from ω and the total number of events.

Table D4
Direction: *South*
Predictor and Total Energy

TYPE = Scaled Percentage	I 12.5	II 37.5	III 0	IV 12.5	V 37.5	Predictor	Total Energy (dB)
3.2 km	1	3	0	3	2	237.5	132.3
8.0 km	1	3	0	5	2	262.5	125.4
16.1 km	1	2	0	5	4	300.0	121.5
24.1 km	1	2	0	3	6	350.0	121.4

Table D5
Percentage of Occurrence of Types of Profiles

Actual Percentage	*Scaled Percentage (Xi)*
0-25%	12.5
26-50%	37.5
51-75%	62.5
76-100%	87.5

Table D6
Results

Column No.	0	1	2	3	4	5	6	7	8
Time Period	=	6:00-8:00 AM			8:00-11:00 AM			6:00-11:00 AM	
Direction	Distance (km)	(dB) Predictor P(d)	(dB) Predicted Total Energy	(dB) Actual Total Energy	(dB) Predictor P(d)	(dB) Predicted Total Energy	(dB) + Energy add columns 2 and 5 to get predicted in column 7	(dB) Predicted Total Energy	(dB) Actual Total Energy
North	3.2	300	116.1	116.0	337.5	119.0		120.8	118.6
	8.0	262.5	104.2	105.4	212.5	100.2		105.7	[illegible]
	16.1	275	98.5	100.0	212.5	93.5		99.7	104.1
	24.1	137.5	83.6	88.8	200	88.6		89.8	94.1
East	5.2	325	118.0	116.3	300	116.1		120.2	119.8
	8.0	325	109.2	108.7	300	107.2		111.3	112.4
	16.1	300	100.5	100.4	237.5	95.5		101.7	104.5
	24.1	212.5	89.6	85.5	150	84.6		90.8	92.7
South	3.2	237.5	111.1	107.0	250	112.1		114.6	108.7
	8.0	262.5	104.2	106.6	200	99.2		105.4	107.9
	16.1	300	100.5	102.8	212.5	93.5		101.3	104.5
	24.1	350	100.5	99.5	300	96.6		102.0	100.2
West	3.2	262.5	113.1	109.1	212.5	109.1		114.6	111.2
	8.0	187.5	98.2	98.2	187.5	98.2		101.2	103.1
	16.1	150	88.5	91.5	187.5	91.5		93.3	96.8
	24.1	212.5	89.6	84.6	150	84.6		90.8	90.0

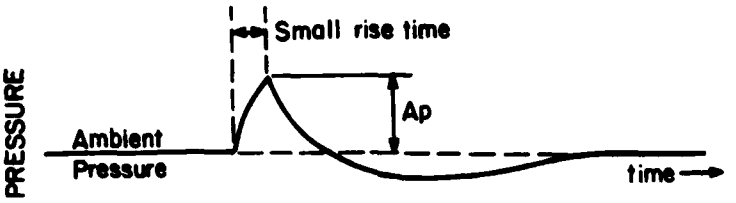

Figure D1. "Pure" blast pressure fluctuations.

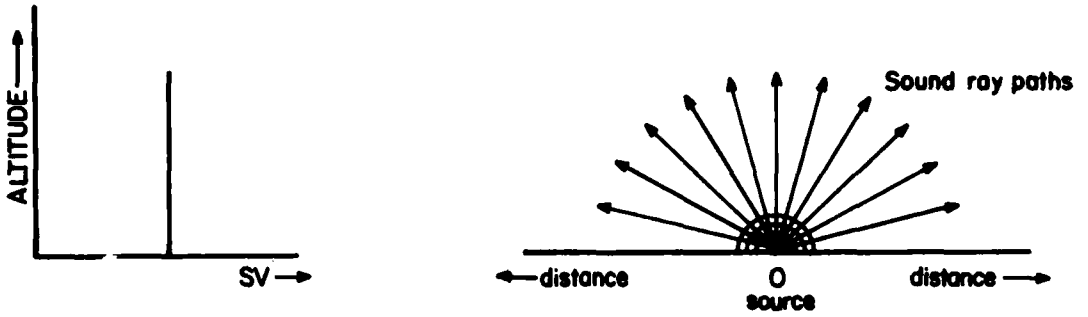

Figure D2. Zero gradient condition model and corresponding ray paths.

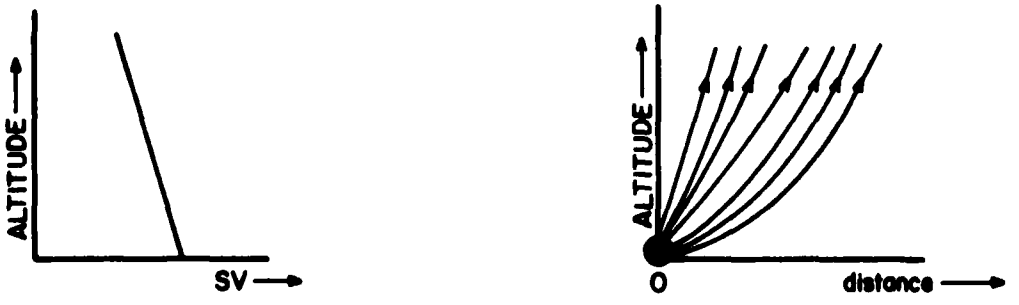

Figure D3. Negative gradient sound velocity profile and corresponding ray paths.

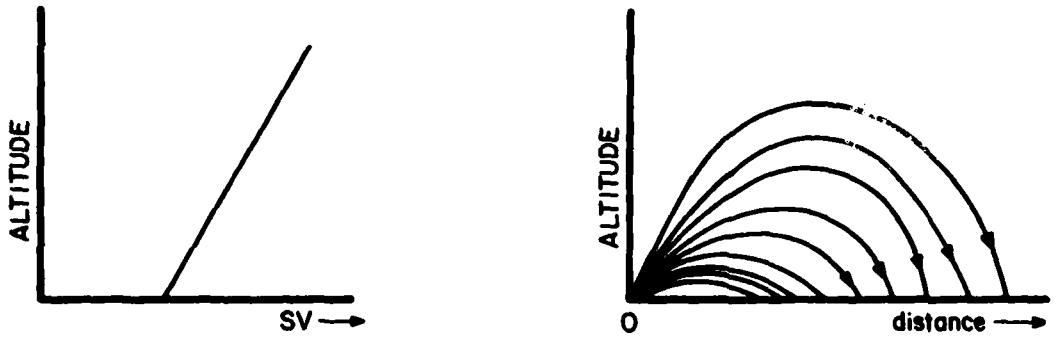

Figure D4. Positive gradient sound velocity profile and corresponding ray paths.

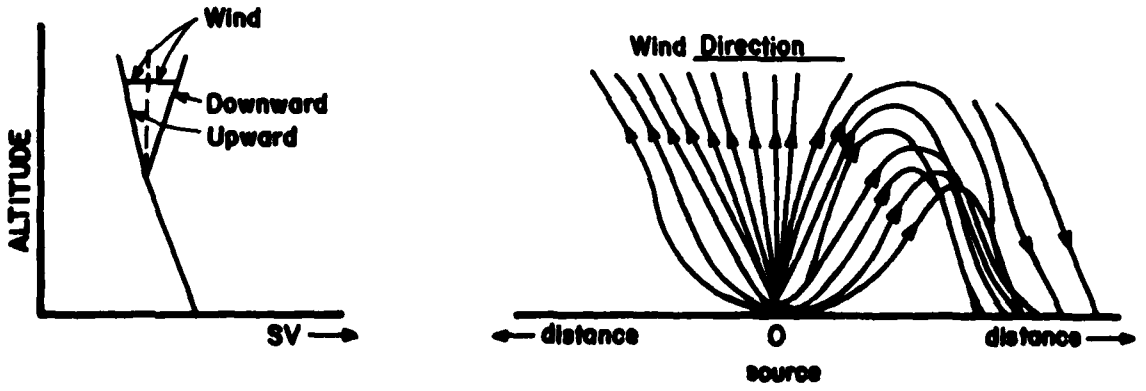

Figure D5. Directional wind effects -- sound velocity profile and ray paths.

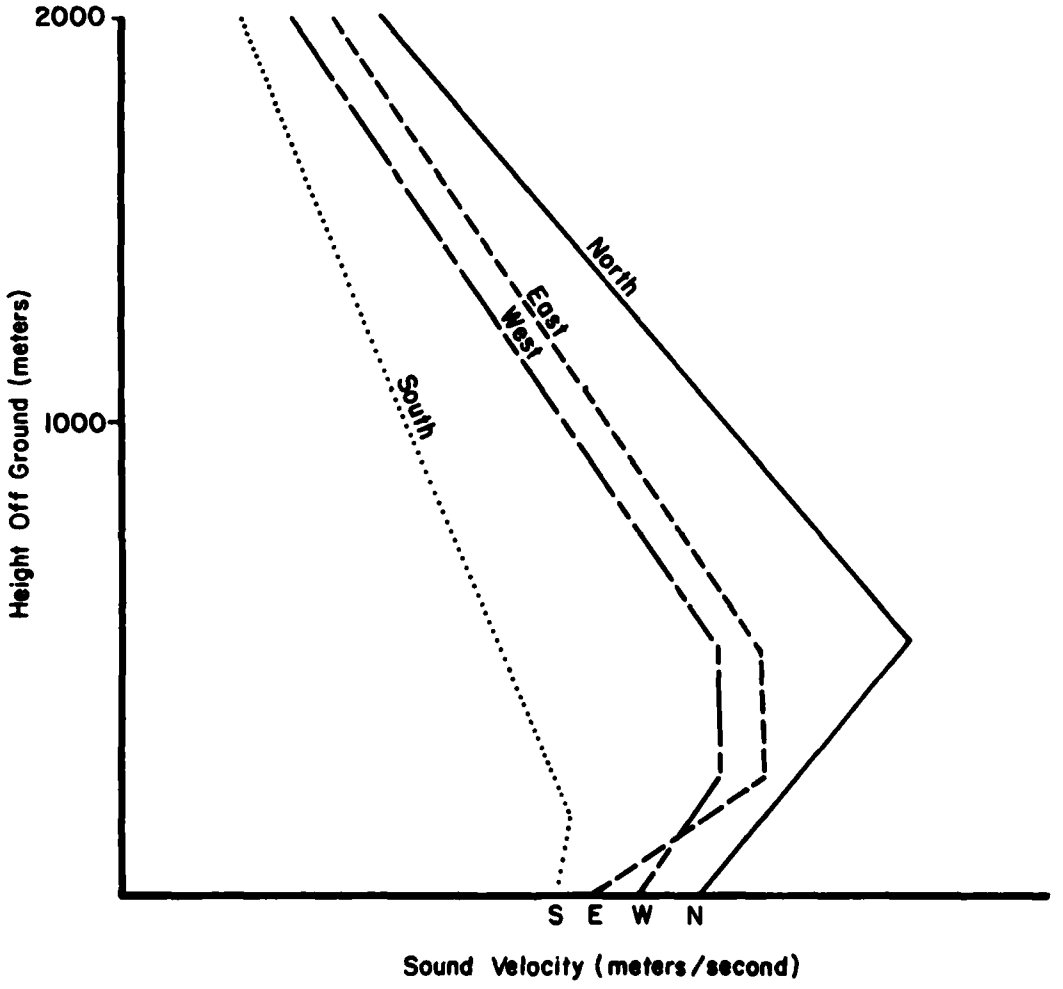

Figure D6. Sound velocity profiles for four directions on example day.

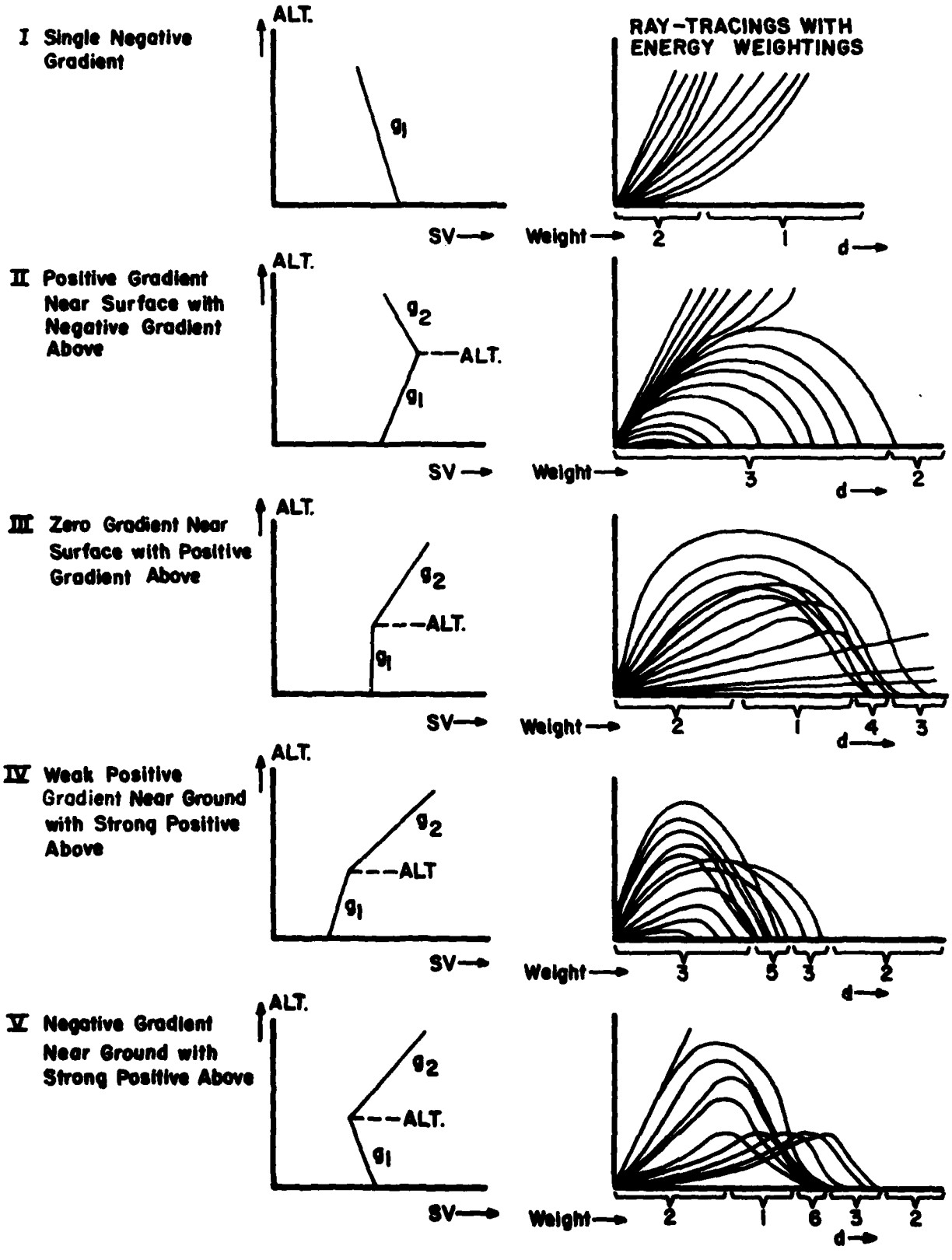

Figure D7. Five sound profile shape categories plus weightings.

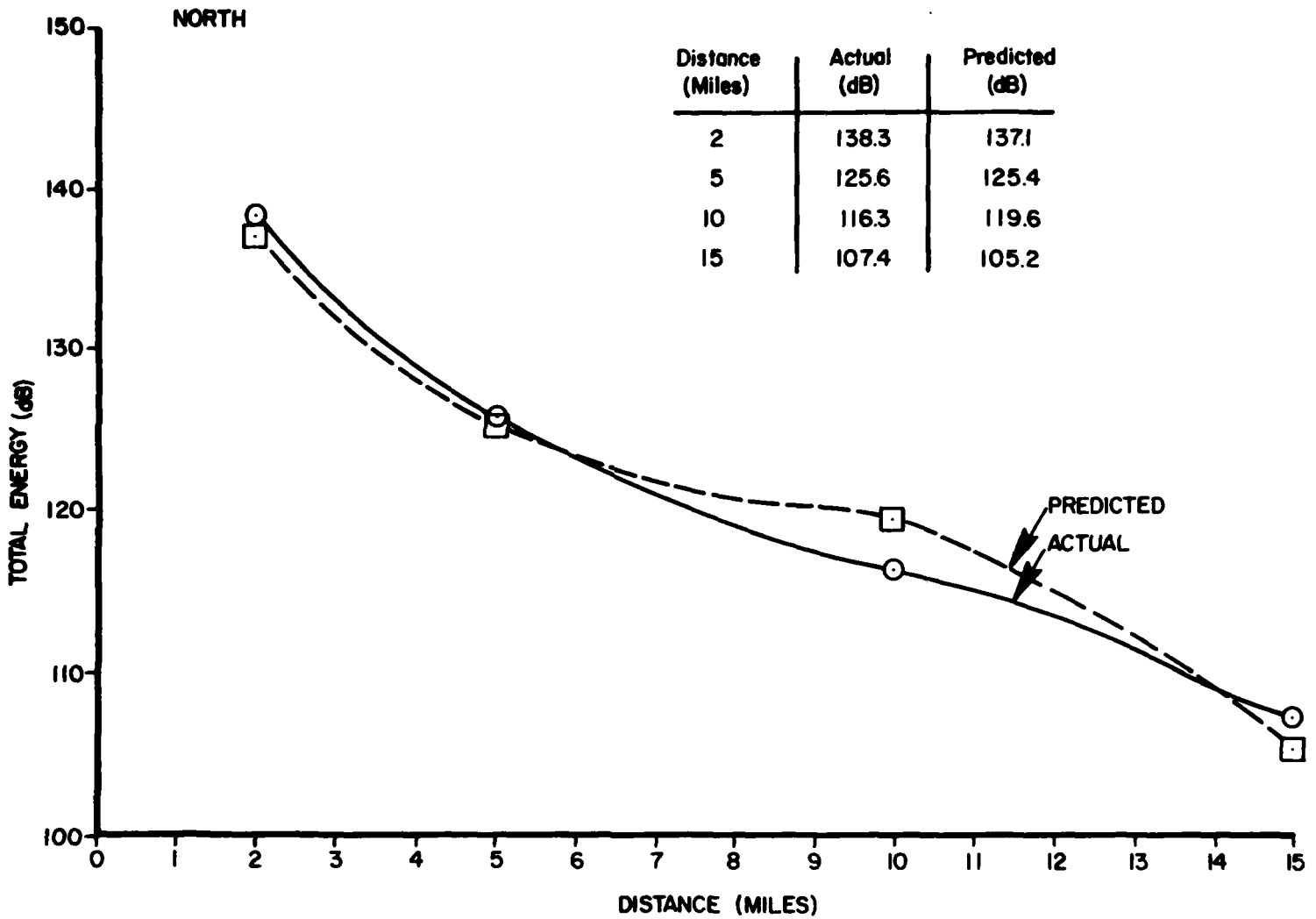

Figure D8. North total energy actual and predicted curves.

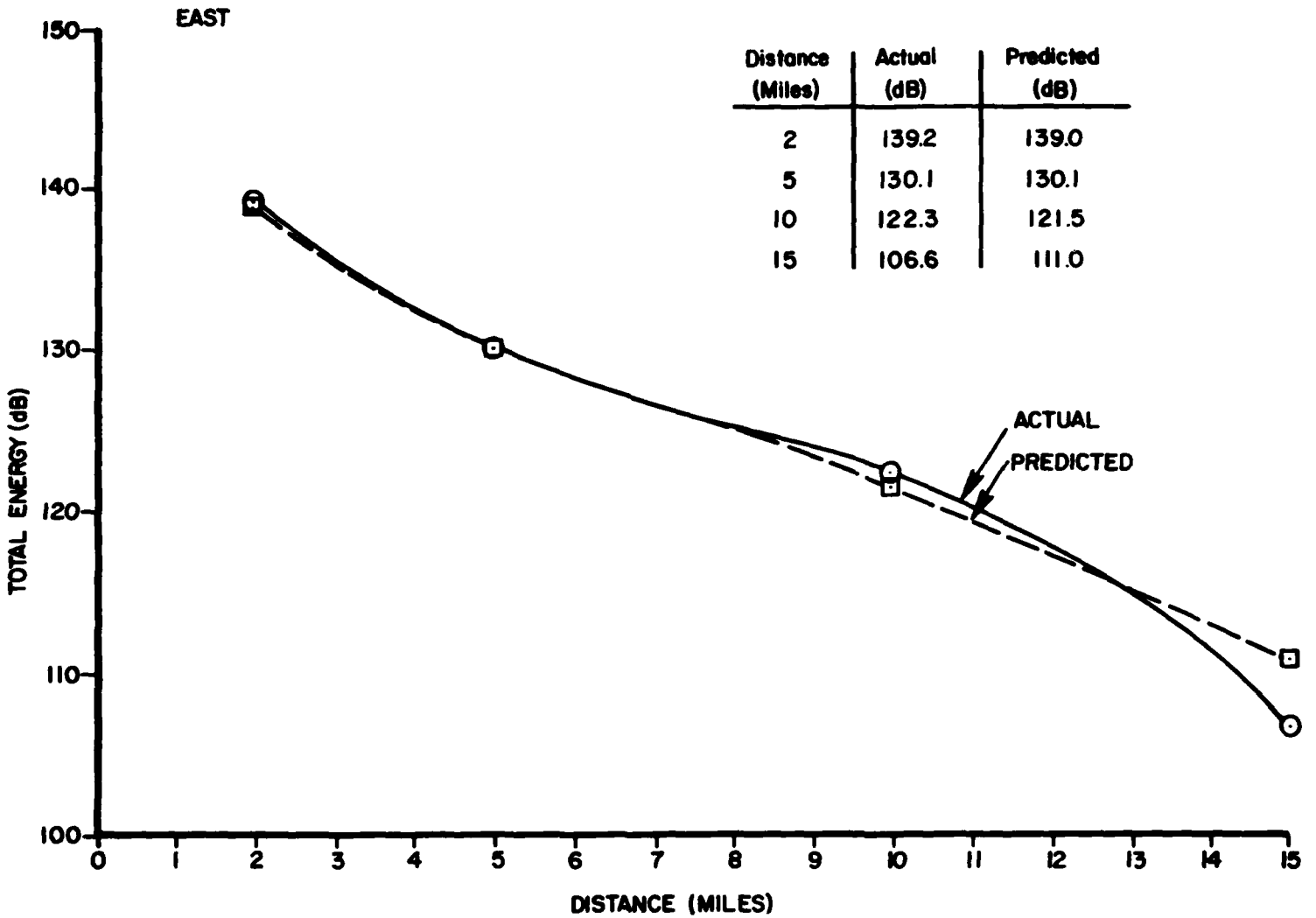

Figure D9. East total energy actual and predicted curves.

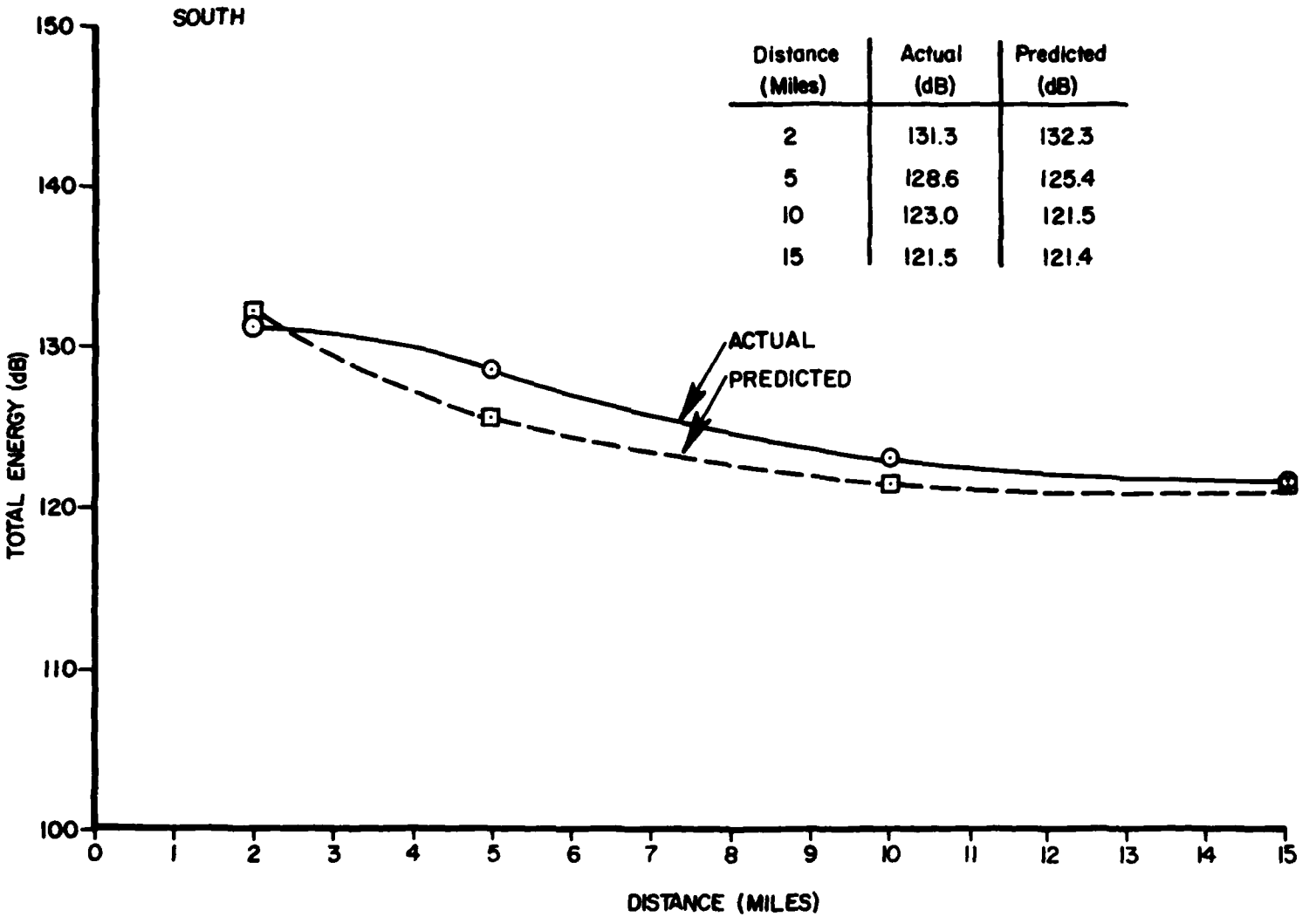

Figure D10. South total energy actual and predicted curves.

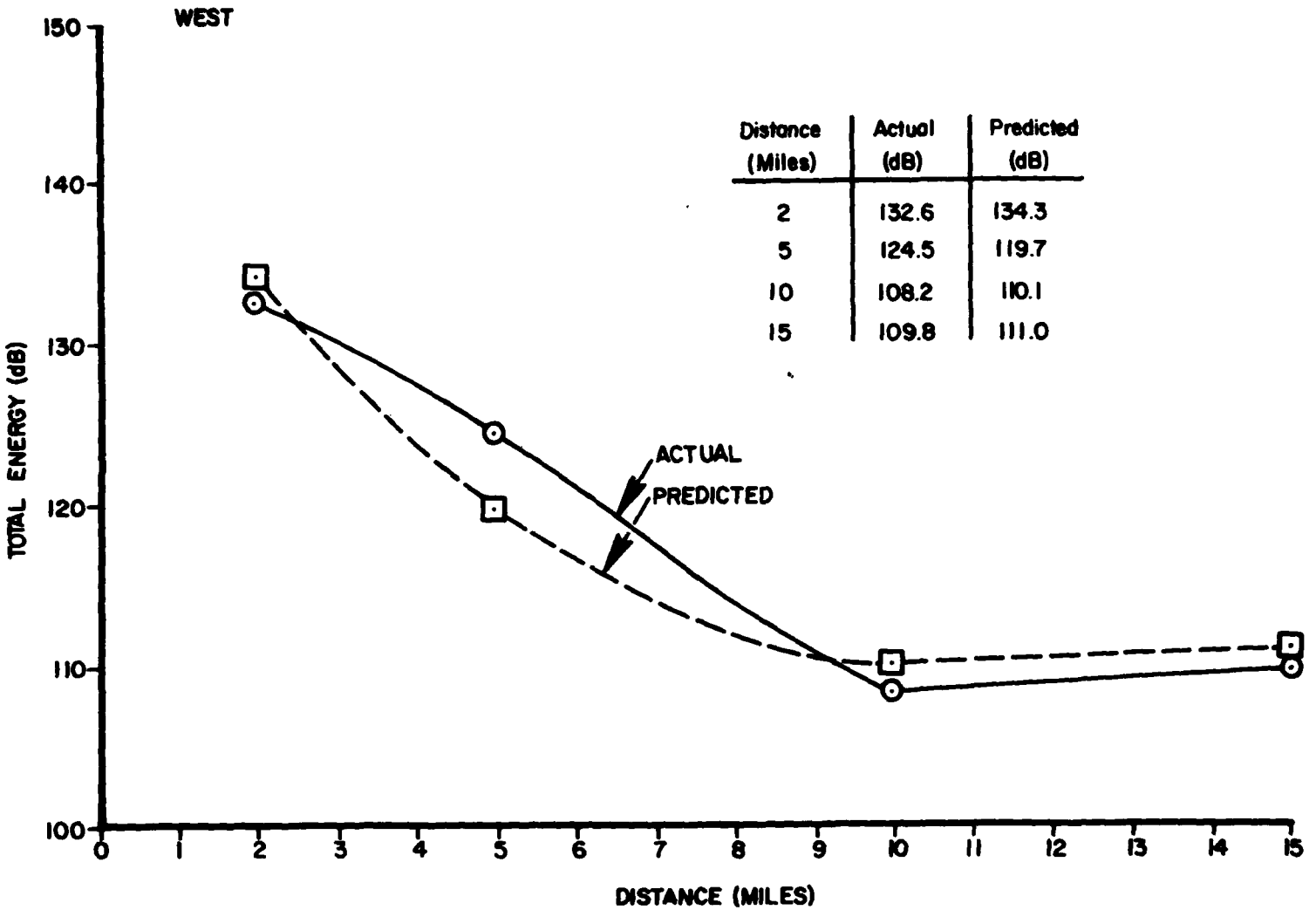

Figure D11. West total energy actual and predicted curves.

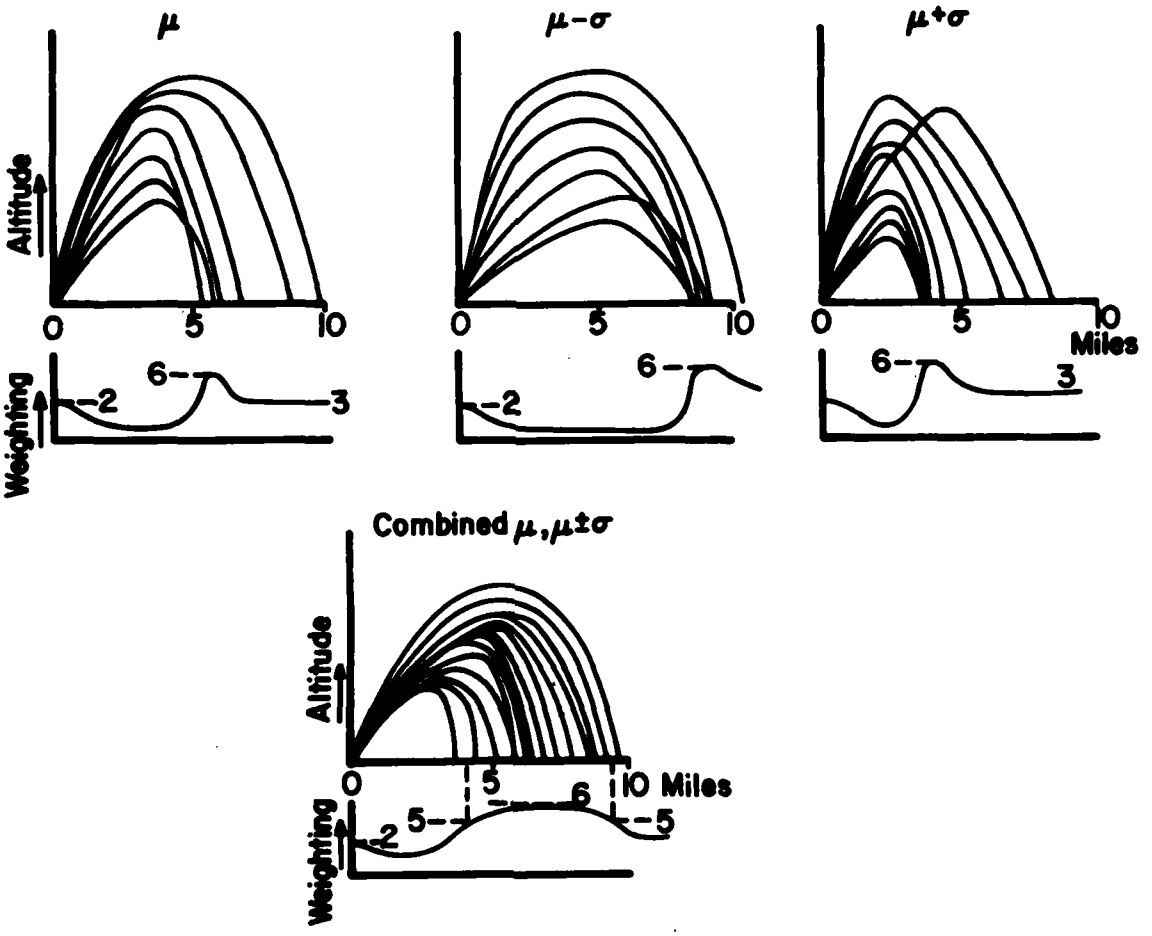

Figure D12. Combination of "mean," "mean + standard deviation" weighting factors.

CERL DISTRIBUTION

Chief of Engineers
ATTN: Tech Monitor
ATTN: DAEN-ASI-L (2)
ATTN: DAEN-CCP
ATTN: DAEN-CW
ATTN: DAEN-CWE
ATTN: DAEN-CWM-R
ATTN: DAEN-CWO
ATTN: DAEN-CWP
ATTN: DAEN-MP
ATTN: DAEN-MPC
ATTN: DAEN-MPE
ATTN: DAEN-MPO
ATTN: DAEN-MPR-A
ATTN: DAEN-RD
ATTN: DAEN-RDC
ATTN: DAEN-RDM
ATTN: DAEN-RM
ATTN: DAEN-ZC
ATTN: DAEN-ZCE
ATTN: DAEN-ZCI
ATTN: DAEN-ZCM

US Army Engineer Districts
ATTN: Library
Alaska
Al Batin
Albuquerque
Baltimore
Buffalo
Charleston
Chicago
Detroit
Far East
Fort Worth
Galveston
Huntington
Jacksonville
Japan
Kansas City
Little Rock
Los Angeles
Louisville
Memphis
Mobile
Nashville
New Orleans
New York
Norfolk
Omaha
Philadelphia
Pittsburgh
Portland
Riyadh
Rock Island
Sacramento
San Francisco
Savannah
Seattle
St. Louis
St. Paul
Tulsa
Vicksburg
Walla Walla
Wilmington

US Army Engineer Divisions
ATTN: Library
Europe
Huntsville
Lower Mississippi Valley
Middle East
Middle East (Rear)
Missouri River
New England
North Atlantic
North Central
North Pacific
Ohio River
Pacific Ocean
South Atlantic
South Pacific
Southwestern

Waterways Experiment Station
ATTN: Library

Cold Regions Research Engineering Lab
ATTN: Library

US Government Printing Office
Receiving Section/Depository Copies (2)

Defense Technical Information Center
ATTN: DDA (12)

Engineering Societies Library
New York, NY

FESA, ATTN: Library

ETL, ATTN: Library

Engr. Studies Center, ATIN: Library

Inst. for Water Res., ATTN: Library

Army Instl. and Major Activities (CONUS)
DARCOM - Dir., Inst., & Svcs.
ATTN: Facilities Engineer
ARRADCOM
Aberdeen Proving Ground
Army Matls. and Mechanics Res. Ctr.
Corpus Christi Army Depot
Harry Diamond Laboratories
Dugway Proving Ground
Jefferson Proving Ground
Fort Monmouth
Letterkenny Army Depot
Natick Research and Dev. Ctr.
New Cumberland Army Depot
Pueblo Army Depot
Red River Army Depot
Redstone Arsenal
Rock Island Arsenal
Savanna Army Depot
Sharpe Army Depot
Seneca Army Depot
Tobyhanna Army Depot
Tooele Army Depot
Watervliet Arsenal
Yuma Proving Ground
White Sands Missile Range

FORSCOM
FORSCOM Engineer, ATTN: AFEN-FE
ATTN: Facilities Engineers
Fort Buchanan
Fort Bragg
Fort Campbell
Fort Carson
Fort Devens
Fort Drum
Fort Hood
Fort Indiantown Gap
Fort Irwin
Fort Sam Houston
Fort Lewis
Fort McCoy
Fort McPherson
Fort George G. Meade
Fort Ord
Fort Polk
Fort Richardson
Fort Riley
Presidio of San Francisco
Fort Sheridan
Fort Stewart
Fort Wainwright
Vancouver Bks.

TRADOC
HQ, TRADOC, ATTN: ATEN-FE
ATTN: Facilities Engineer
Fort Belvoir
Fort Benning
Fort Bliss
Carlisle Barracks
Fort Chaffee
Fort Dix
Fort Eustis
Fort Gordon
Fort Hamilton
Fort Benjamin Harrison
Fort Jackson
Fort Knox
Fort Leavenworth
Fort Lee
Fort McClellan
Fort Monroe
Fort Rucker
Fort Sill
Fort Leonard Wood

INSCOM - Ch, Instl. Div.
ATTN: Facilities Engineer
Vint Hill Farms Station
Arlington Hall Station

WESTCOM
ATTN: Facilities Engineer
Fort Shafter

MDW
ATTN: Facilities Engineer
Cameron Station
Fort Lesley J. McNair
Fort Myer

HSC
HQ USAHSC, ATTN: HSLO-F
ATTN: Facilities Engineer
Fitzsimons Army Medical Center
Walter Reed Army Medical Center

USACC
ATTN: Facilities Engineer
Fort Huachuca
Fort Ritchie

MTMC
HQ, ATTN: MTMC-SA
ATTN: Facilities Engineer
Oakland Army Base
Bayonne MOT
Sunny Point MOT

US Military Academy
ATTN: Facilities Engineer
ATTN: Dept of Geography & Computer Science

USAES, Fort Belvoir, VA
ATTN: ATZA-DTE-EM
ATTN: ATZA-DTE-SU
ATTN: Engr. Library

Chief Inst. Div., I&SA, Rock Island.

USA ARRCOM, ATTN: Dir., Instl & Svc
TARCOM, Fac. Div.
TECOM, ATTN: DRSTE-LG-F
TSARCOM, ATTN: STSAS-F
NARAD COM, ATTN: DRDNA-F
AMMRC, ATTN: DRXMR-WE

HQ, XVIII Airborne Corps and Ft. Bragg
ATTN: AFZA-FE-EE

HQ, 7th Army Training Command
ATTN: AETTG-DEH (5)

HQ USAREUR and 7th Army
ODCS/Engineer
ATTN: AEAEN-EH (4)

V Corps
ATTN: AETVDEH (5)

VII Corps
ATTN: AETSDEH (5)

21st Support Command
ATTN: AEREH (5)

US Army Berlin
ATTN: AEBA-EN (2)

US Army Southern European Task Force
ATTN: AESE-ENG (5)

US Army Installation Support Activity Europe
ATTN: AEUES-RP

8th USA, Korea
ATTN: EAFE
Cdr, Fac Engr Act (8)
AFE, Yongsan Area
AFE, 2D Inf Div
AFE, Area II Spt Det
AFE, Cp Humphreys
AFE, Pusan
AFE, Taegu

DLA ATTN: DLA-WI

USA Japan (USARJ)
Ch, FE Div, AJEN-FE
Fac Engr (Honshu)
Fac Engr (Okinawa)

ROK/US Combined Forces Command
ATTN: EUSA-HHC-CFC/Engr

416th Engineer Command
ATTN: Facilities Engineering

Norton AFB
ATTN: AFRCE-MX/DEE

ENA Team Distribution

USA ARRADCOM
ATTN: DRDAR-LCA-OP

Director of Facilities Engr
Miami, FL 34004

HQ US Army Materiel, DARCOM
ATTN: DRCPA-E/E. Proudman
ATTN: DRCIS-A
Alexandria, VA 22333

HQDA (SGRD-EDE)

Chief of Engineers
ATTN: DAEN-MPC-E/D. Spivey
ATTN: DAEN-MPO-B
ATTN: DAEN-MPR
ATTN: DAEN-MPZ-A
ATTN: DAEN-RDL
ATTN: DAEN-MPE-B/W. B. Holmes
ATTN: DAEN-MPC-E/P. Van Parys
ATTN: DAEN-MPE-I/F. P. Beck (2)
ATTN: DAEN-MPE-I/J. Halligan
ATTN: DAEN-ZCE-O/E. Herndon (2)

Ft. Belvoir, VA 22060
ATTN: Kingman Bldg, Library
ATTN: Canadian Liaison Officer (2)

DFAE Envir Quality Section
ATTN: Mike Halla
Ft. Carson, CO 80192

Ft. Leavenworth, KS 66027
ATTN: ATZLCA-SA

Ft. Monroe, VA 23651
ATTN: ATEN-FE-E/D. Dery
ATTN: James L. Aikin, Jr.
ATTN: Chief, Envr Branch
ATTN: ATEN-AD (3)

Ft. McPherson, GA 30330
ATTN: AFEN-FEB
ATTN: Robert Jarrett

Ft. Detrick, MD 21701
ATTN: LTC LeRoy H. Reuter

Ft. Rucker, AL 36360
ATTN: Robert T. Camp, Jr.
ATTN: CPT J. Patterson

USA-WES
ATTN: Jack Stoll/WESSE

6th US Army
ATTN: AFKC-EN

7th US Army
ATTN: AETTM-HRD-EHD

Aberdeen Proving Ground, MD 21005
ATTN: DRDAR-BLL/Schmidt/Uahl
ATTN: STEAP-MT-E/Conley
Human Engineering Laboratory
ATTN: J. E. Weisz/AMZHE
ATTN: George Garinther
Army Environmental Hygiene Agency
ATTN: CPT George Luz/BioAcoustics

US Army Engineer District
New York
ATTN: Chief, Design Br
Philadelphia
ATTN: Chief, NAPEN-E
Baltimore
ATTN: Chief, Engr Div
Norfolk
ATTN: Chief, NAOEN-D
Huntington
ATTN: Chief, ORHED
Wilmington
ATTN: Chief, SAWEN-D

US Army Engineer District
Savannah
ATTN: Chief, SASAS-L
Mobile
ATTN: Chief, SAMEN-D
Louisville
ATTN: Chief, Engr Div
St. Paul
ATTN: Chief, ED-D
Chicago
ATTN: Chief, NCCPE-PES
Rock Island
ATTN: Chief, Engr Div
St. Louis
ATTN: Chief, ED-D
Omaha
ATTN: Chief, Engr Div
New Orleans
ATTN: Chief, LMNED-DG
Little Rock
ATTN: Chief, Engr Div
Tulsa
ATTN: Chief, Engr Div
Ft. Worth
ATTN: Chief, SWFED-D
ATTN: Bill G. Daniels
ATTN: Royce W. Mullens, Water Resource Planning
San Francisco
ATTN: Chief, Engr Div
Sacramento
ATTN: Chief, SPKED-D
Far East
ATTN: Chief, Engr Div
Seattle
ATTN: Chief, EN-DB-ST
Walla Walla
ATTN: Chief, Engr Div
Alaska
ATTN: Chief, NPASA-R

US Army Engineer Division
New England
ATTN: Chief, NEDED-T
North Atlantic
ATTN: Chief, NADEN-T
Middle East (Rear)
ATTN: Chief, MEDED-T
South Atlantic
ATTN: Chief, SADEN-TS
Huntsville
ATTN: Chief, HNDED-CS
ATTN: Chief, HNDED-SR
Ohio River
ATTN: Chief, Engr Div
Missouri River
ATTN: Chief, MRDED-T
Southwestern
ATTN: Chief, SWDED-T
South Pacific
ATTN: Chief, SPDED-TG
Pacific Ocean
ATTN: Chief, Engr Div
North Pacific
ATTN: Chief, Engr Div

National Defense HQDA
Director General of Construction
Ottawa, Ontario, Canada K1A OK2

Division of Building Research
National Research Council
Ottawa, Ontario, Canada K1A OR6

Airports and Construction Services Dir
Technical Information Reference Centre
Ottawa, Ontario, Canada K1A ON8

McClellan AFB, CA 95652
2852 APG/DE

AF/PREEU
Bolling AFB, DC 20332

Patrick AFB, FL 32925
ATTN: XRQ

AFESC/PRI
Tyndall AFB, FL 32403

Wright-Patterson AFB, OH 45433
ATTN: Dr. H. Von Gierke
ATTN: Jerry Speakman
ATTN: LTC D. Johnson

Naval Undersea Center, Code 401
ATTN: Bob Gales
ATTN: Dr. Robert Young, Code 51212B
San Diego, CA 92152

Naval Air Station
ATTN: Ray Glass/Code 661
North Island, CA 92135

US Naval Oceanographic Office
Bay St. Louis, MS 39522

Naval Surface Weapons Center
ATTN: N-43/Pater
Dahlgren, VA 22485

Naval Air Systems Command
WASH DC 20360

NAVFAC
ATTN: Code 04
ATTN: David Kurtz/Code 2013C
Alexandria, VA 22332

Port Hueneme, CA 93043
ATTN: Library (Code L08A)

Washington, DC
ATTN: Building Research Advisory Board
ATTN: Transportation Research Board
ATTN: Library of Congress (2)
ATTN: Dept of Transportation Library

Federal Aviation Administration
ATTN: H. B. Safeer, Chief
Envr Policy Div

National Bureau of Standards
ATTN: Dan R. Flynn

Bureau of National Affairs
ATTN: Fred Blosser, RM 462

Office of Noise Abatement
ATTN: Gordon Banerian

Dept of Housing and Urban Development
ATTN: George Winzer, Chief Noise Abatement Program

NASA
ATTN: J. Fields
ATTN: H. Hubbard

EPA Noise Office
ATTN: Al Hicks, Rm 2113
ATTN: Dr. Kent Williams, Rm 109
ATTN: Tom O'Hare, Rm 907G

EPA Region III Noise Program
ATTN: Pat Anderson

Illinois EPA
ATTN: DNPC/Greg Zak
ATTN: Bob Hellweg

EPA
ATTN: AW-471/C. Caccavari
ATTN: AW-471/H. Nozick
ATTN: R. Marrazzo
ATTN: W. Sperry
ATTN: J. Goldstein
ATTN: D. Gray
ATTN: D. Mudarri
ATTN: R. Hayman
ATTN: Robert A. Simmons
ATTN: B. Manns

USA Logistics Management Center
Bldg 12028
ATTN: MAJ K. Valentine

Federal Highway Administration
Region 15
ATTN: William Bowlby

128
+30

Blast Noise Prediction/by Paul D. Schomer...et al. -- Champaign, IL : Construction Engineering Research Laboratory ; available from NTIS, 1981.
2v. (Technical report ; N-98)

Contents: v.1. Data bases and computational procedures. -- v.2. BNoise 3.2 computer program description and program listing.

1. Noise pollution. 2. Ordnance - noise 3. BNOISE (computer program) I. Schomer, Paul D. II. Little, Lincoln L. III. Effland, David L. IV. Pawlowska, Violet I. V. Roubik, Steven C. VI. Series: U.S. Army Construction Engineering Research Laboratory. Technical report ; N-98.